Elastic materials for tissue engineering applications

Acta Biomaterialia 79 (2018) 60–82

Contents lists available at ScienceDirect

Acta Biomaterialia

journal homepage: www.elsevier.com/locate/actabiomat

Review article

Elastic materials for tissue engineering applications: Natural, synthetic, and hybrid polymers

Anna M.J. Coenen [a], Katrien V. Bernaerts [a], Jules A.W. Harings [a], Stefan Jockenhoevel [a,b], Samaneh Ghazanfari [a,*]

[a] Aachen-Maastricht Institute for Biobased Materials (AMIBM), Faculty of Science and Engineering, Maastricht University, Brightlands Chemelot Campus, Urmonderbaan 22, 6167 RD Geleen, The Netherlands
[b] Department of Biohybrid & Medical Textiles (BioTex), AME-Helmholtz Institute for Biomedical Engineering, RWTH Aachen University, Forckenbeckstraβe 55, 52072 Aachen, Germany

ARTICLE INFO

Article history:
Received 26 February 2018
Received in revised form 3 August 2018
Accepted 21 August 2018
Available online 28 August 2018

Keywords:
Elastin
Extracellular matrix
Tissue engineering
Mechanical functionality
Elasticity

ABSTRACT

Elastin and collagen are the two main components of elastic tissues and provide the tissue with elasticity and mechanical strength, respectively. Whereas collagen is adequately produced *in vitro,* production of elastin in tissue-engineered constructs is often inadequate when engineering elastic tissues. Therefore, elasticity has to be artificially introduced into tissue-engineered scaffolds. The elasticity of scaffold materials can be attributed to either natural sources, when native elastin or recombinant techniques are used to provide natural polymers, or synthetic sources, when polymers are synthesized. While synthetic elastomers often lack the biocompatibility needed for tissue engineering applications, the production of natural materials in adequate amounts or with proper mechanical strength remains a challenge. However, combining natural and synthetic materials to create hybrid components could overcome these issues. This review explains the synthesis, mechanical properties, and structure of native elastin as well as the theories on how this extracellular matrix component provides elasticity *in vivo*. Furthermore, current methods, ranging from proteins and synthetic polymers to hybrid structures that are being investigated for providing elasticity to tissue engineering constructs, are comprehensively discussed.

Statement of Significance

Tissue engineered scaffolds are being developed as treatment options for malfunctioning tissues throughout the body. It is essential that the scaffold is a close mimic of the native tissue with regards to both mechanical and biological functionalities. Therefore, the production of elastic scaffolds is of key importance to fabricate tissue engineered scaffolds of the elastic tissues such as heart valves and blood vessels. Combining naturally derived and synthetic materials to reach this goal proves to be an interesting area where a highly tunable material that unites mechanical and biological functionalities can be obtained.

Abbreviations: ECM, Extracellular matrix; GAGs, Glycosaminoglycans; ELN-gene, Elastin gene; RER, Rough endoplasmic reticulum; EBP, Elastin-binding protein; GAS, Galacto-sugars; LCST, Lower critical solution temperature; T_g, Glass transition temperature; ELAC, Electrochemically aligned collagen; ELP, Elastin-like polypeptide; PLA, Poly (lactic acid); PEG, Poly(ethylene glycol); PGS, Poly(glycerol-co-sebacate); POC, Poly(1,8-octanediol-co-citrate); PLLA, poly(L-lactic acid); PU, Polyurethane; PCL, Poly(ε-caprolactone); PHA, Poly(hydroxyalkanoate); P4HB, Poly(4-hydroxybutyrate); GelMA, Methacrylated gelatinl; PHB, Poly(3-hydroxybutyrate); PHBHHx, Poly(3-hydroxybutyrate-co-3-hydroxyhexanoate); PLGA, Poly(lactic-co-glycolic acid); PGCL, Poly(glycolide-co-ε-caprolactone); PTMC, poly(1,3-trimethylene carbonate); PA, Polyacrylamides; PAA, Poly(acrylic acid); PGA, poly(glycerol adipate); PSBS, Poly(styrene-butadienestyrene); PSEBS, Poly(styrene-ethylene-butadiene-styrene); LDLA, L,D-lactic acid; PLCL, Poly (l-lactide-co-ε-caprolactone); PGLCL, poly(glycolide-co-L-lactide-co-ε-caprolactone); AP, Aniline pentapeptide; HDI, Hexamethylene diisocyanate; PDMS, Polydimethylsiloxane; PIBMD, Poly(isobutyl-morpholinedione); SELP, Silk elastin-like polypeptides; AKELP, Mimic of the hydrophilic-, alanine-, and lysine-rich part of tropoelastin; PNIPAAm, Poly(N-isopropylacrylamide); PLA-HEMA, Polylactide-2-hydroxyethyl methacrylate; OEGMA, Oligo(ethylene glycol); PNPHO, A complex water-soluble polymer containing PNIPAAm, PLA/HEMA, and OEGMA; PEGDA, Poly(ethylene glycol) diacrylate.

* Corresponding author.
E-mail address: ghazanfari@maastrichtuniveristy.nl (S. Ghazanfari).

https://doi.org/10.1016/j.actbio.2018.08.027
1742-7061/

Contents

1. Introduction

Tissue engineering is a fast growing field that aims at generating functional constructs that mimic the structure and properties of the extracellular matrix (ECM) of the native tissues. Although many studies have been carried out in the field of tissue engineering, the number of constructs that are brought to the clinics is still limited [1,2]. The limited clinical translation of engineered tissues is mainly because many applications such as heart valve and blood vessel replacements require the construct to be mechanically functional upon implantation [3]. Thus, understanding the functional mechanical properties of native tissues and how to mimic these properties in an engineered construct is essential [4–7].

Native tissues consist of two major components: cells and the ECM. The ECM consists of nonfibrous macromolecules such as glycosaminoglycans (GAGs) and fibrous components such as elastin. Although nonfibrous components are present in a relatively low content in elastic tissues, they play an important role in the proper mechanical functionality of these tissues [8]. In heart valves, for example, the GAG-rich layer is able to absorb the shocks during opening and closing of the valve [4]. Fibrous components, mostly collagen and elastin, are the major elements that provide mechanical functionality to elastic tissues. Collagen fibers provide strength and structural support to the tissue. Elastin, however, provides elasticity and is therefore mostly present in elastic tissues such as lungs, heart valves, and blood vessels [2,9]. To engineer a tissue *in vitro*, scaffolds are designed to provide initial mechanical stability to the construct and to allow the cells to produce the proper amount of the ECM with time. While the amount of collagen produced by the cultured cells is abundant, the amount of elastin is limited [10–12]. Therefore, it is essential to artificially introduce elasticity into the scaffold materials [13,14].

Elasticity can be tailored to the scaffold by using native elastin derivatives [2] or synthetic elastomers [9]. While the use of native elastin proves to be difficult owing to its large batch-to-batch variations [15], synthetic materials, which have a high tunability, may cause problems regarding the biological functionalities, especially by hindering cell adhesion [16]. Combining different natural and synthetic materials with different functionalities, to form hybrid-like structures, can address the limitations of both native elastin and synthetic elastomers and thus offer a promising future approach for the engineering of elastic tissues.

In this review, various elastic materials used for tissue engineering applications are discussed. First, elastin synthesis, *in vivo* procedure for fiber assembly, and occurrence of elastin in different tissues are explained. Next, the current available elastic materials from biological, recombinant, and synthetic sources for tissue engineering purposes are discussed. Finally, hybrid materials, as promising candidates for tissue engineering applications, are highlighted.

2. Native elastin

2.1. Elastin biosynthesis

Cells produce elastin as the precursor tropoelastin before it is transported outside the cells [17]. After alignment through coacervation, the protein is crosslinked to form the mature elastin [18]. The majority of the elastin synthesis takes place in the late fetal and early neonatal stage [11]. For humans, elastin production starts between weeks 17 and 19 of pregnancy and continues into early childhood before slowing down [14,19]. In line with this, Johnson *et al.* indicated that aortic cultures from 1 to 3 day old chickens showed a decreasing trend of elastin synthesis with time [20]. They linked this decreasing trend to the half-life time of elastin mRNA, which decreased from 25 h in 1 day old chickens to only 7 h in 8 week old chickens [20]. Because elastin has a half-life time of approximately 70 years, during which it can go through billions of extension and relaxation cycles without losing its function [2], production and remodeling of elastin is not essential during adulthood except in the case of damage to the elastin fibers due to an injury. The elastin fibers produced in the case of injury are disorganized and therefore do not have mechanical functionalities same as those of the elastin produced during early life [11]. Several exogenous factors influence the production of elastin after injury, such as tumor necrosis factor-a, interleukin 1b, insulin-like growth-factor-1, and transforming growth factor [21].

The formation of mature elastic fibers, also known as elastogenesis, starts with the translation of the elastin gene (ELN gene) inside the cell nucleus and its transcription into tropoelastin in the rough endoplasmic reticulum (RER) (Fig. 1A, I) [22]. The gene coding for tropoelastin is a single coding gene that can have alternative splicing, thereby resulting in different isoforms of tropoelastin [17]. In humans, the resulting tropoelastins possess a weight of approximately 70 kDa [23] and consist of alternating parts: a hydrophilic part containing predominantly alanine and lysine, known as the crosslinking domain and a hydrophobic part containing the repeating sequence of Val-Pro-Gly-Val-Gly (Fig. 1B) [24].

Inside the cells, tropoelastin is bound to a chaperone, an elastin-binding protein (EBP), that prevents intracellular coacervation. Coacervation is a conformational reorganization of molecules in a

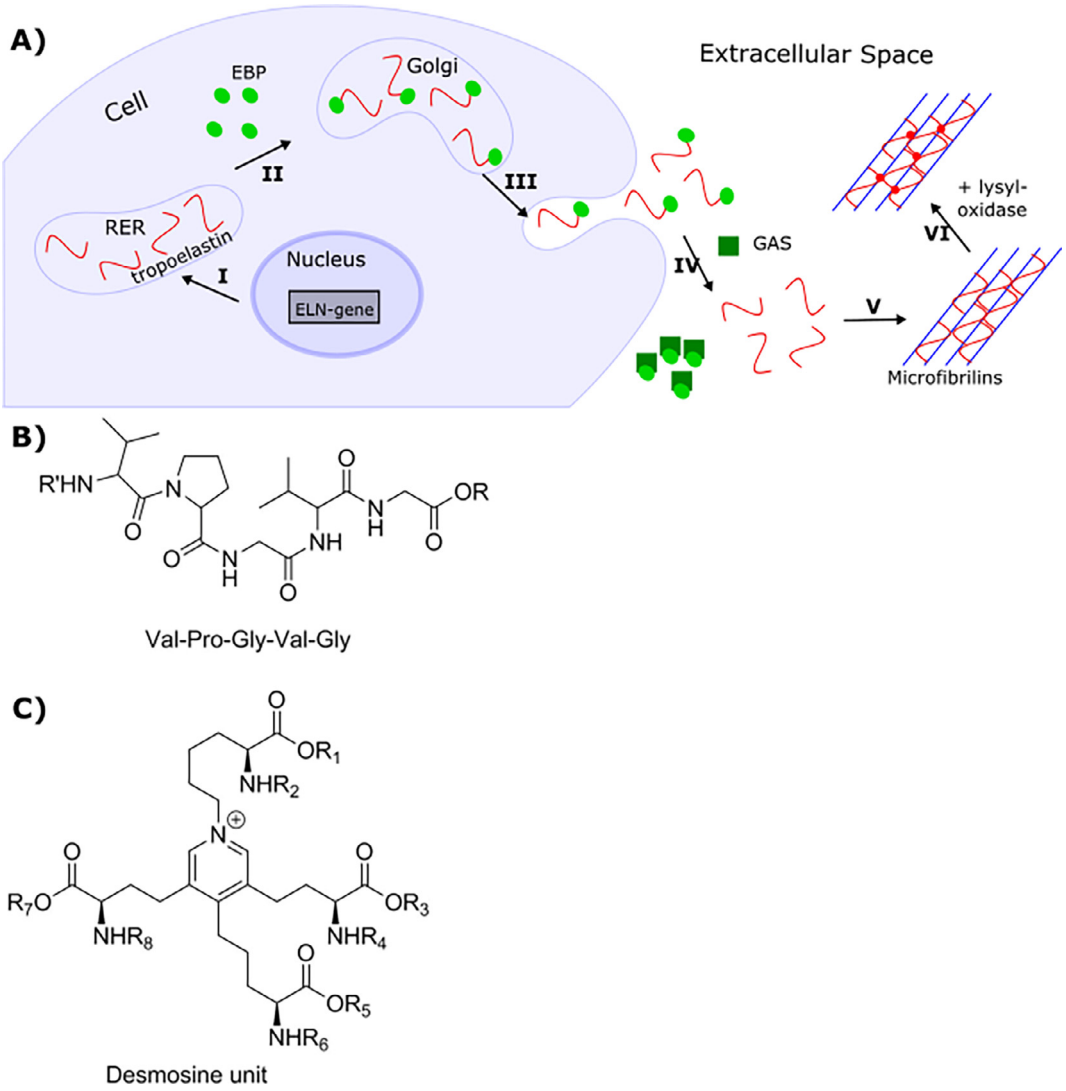

Fig. 1. A) Elastogenesis (adapted from Debelle and Tamburro [23] and Nivison-Smith and Weiss [22]): i) translation of the ELN gene, ii) transcription into tropoelastin and association with EBP to prevent coacervation, iii) transportation of tropoelastin-EBP to the extracellular space by the Golgi apparatus, iv) interaction between EBP and GAS to release tropoelastin, v) coacervation of tropoelastin guided by microfibrillin, and vi) crosslinking of tropoelastin into mature elastin by lysyl- oxidase. B) Chemical structure of the repeating pentapeptide present in the hydrophobic part of tropoelastin. C) Chemical representation of the crosslink between tropoelastin moieties.

solution upon increasing the temperature or salt concentration (Fig. 1A, II) [25]. After secretion of tropoelastin by the Golgi apparatus into the extracellular space, the EBP interacts with the galacto-sugars (GAS), and this results in the release of tropoelastin (Fig. 1A, III–IV). Coacervation is then guided by the microfibrils, which are already present and play an important role in the alignment of the tropoelastin (Fig. 1A, V) [23,26]. After the tropoelastins are aligned, the lysine moieties in the protein will be subsequently deaminated and oxidized by lysyl oxidase in the presence of Cu^{2+} to form allysines and before crosslinking to form (iso)desmosine (Fig. 1C) [18,23,27,28]. The crosslinking procedure leads to the formation of mature insoluble elastin (Fig. 1A, VI) [2].

2.2. (Tropo)elastin properties

One of the important characteristics of tropoelastin is its coacervation behavior, also known as lower critical solution temperature (LCST) behavior [25]. This behavior is vital in obtaining properly aligned elastin fibers during elastin biosynthesis (Fig. 1A, V). The purely entropic coacervation process occurs because water is released from the chain, thus making it thermodynamically favorable for the polymers, proteins in this case, to conformationally reorganize and aggregate [29]. The coacervation temperature of materials is dependent on pH, salt concentration, molecular structure, and concentration of the material. For tropoelastin, coacervation occurs under physiological conditions, as discussed in Section 2.1.

Within the cross-linked structures of mature elastin, the tropoelastin moieties are quite flexible and show elastic behavior. A good indicator for the elasticity of polymers at a certain temperature is their glass transition temperature (T_g). The polymer is in a rubbery state with more elasticity above the T_g, whereas it is usually brittle in the glassy state below the T_g. The T_g of dry elastin is approximately 200 °C, but upon increasing the hydration to 30%, the T_g significantly decreases to only 30 °C, thus indicating that elastin shows elastic behavior only in its hydrated state [2].

The necessity of water for elasticity implies that water plays an important role for conferring elasticity [30]. One theory states that when elastin swells in water, water molecules distribute through the elastin network. In this case, interaction of water molecules with the polar peptide groups mediates macromolecular conformational and translational segmental motion, thus making

the network more flexible [23]. In the relaxed state, water inside the elastin network interacts strongly with the bulk water surrounding the network. When the network is extended, the bulk water is excluded and accounts for a loss in entropy. The influence of water, owing to its plasticizing effect, can also be explained by the large amount of β-turns found in elastin. The sliding behavior of one residue in these β-turns toward the C-terminus leads to intrinsic entropy owing to its dynamic nature [23].

Different theories about the exceptional mechanism of elasticity in elastin are based on the structure of the hydrophobic domains. One theory, based on enthalpic forces, states that when the protein is extended, the hydrophobic side chains of elastin are exposed on the outside. Consequently, the overall energy in the system increases enthalpically, thus supporting the conventional entropic diving force to recoil [14]. It is important to note that all described theories on the elasticity mechanisms in elastin indicate that the relaxed state is more hydrated, more chaotic or unstructured, and more mobile than the extended state.

The Young's modulus is an indication for the stiffness of materials and is derived by generating the stress–strain curve. Young's moduli of elastin reported in the literature differ substantially. For example, a study on aortic elastin fibers purified by autoclaving and measured in a water bath (a hydrated environment) showed a Young's modulus of 0.81 MPa and a maximum extension of approximately 100% [31]. However, purified single elastin fibers from ligaments showed a Young's modulus of 1–1.2 MPa and an extension of 100–200%; the results were dependent on the purification method [32–34]. Other sources, on the other hand, reported a much lower Young's modulus of 300–600 kPa with similar extensions of 100–220% [14,35]. An explanation of the discrepancy between Young's moduli can be related to the differences in the source of elastin as well as the measurement conditions. Because elastin has a viscoelastic nature, the mechanical response is time and temperature dependent, meaning that the strain rate could influence the resulting value. Furthermore, environmental conditions such as relative humidity could also influence the outcome of mechanical tests [36]. The above-mentioned parameters should be considered for a proper comparison of the results of different studies.

For elastic tissue engineering applications, the toughness of the material is not the only important mechanical characteristic, as it does not prove the reversible extensibility, which is known as elasticity. Therefore, it is important to generate the repetitive stress–strain curves. In biological tissues, the curves generated consist of not one but two successive regions, which allow the material to return to its original state under larger strain. The first part of the curve, called the toe region, represents the phase where the undulated collagen fibers are stretched to an extended state, and the second part represents the phase where uncrimped collagen fibers are stretched. Recruitment pattern and alignment of collagen fibers, when the tissue is extended, primarily define the trend of such curves. Finally, the shape of the curves is dependent on the relative quantitative proportion, three-dimensional arrangement, and the mechanical properties of collagen and elastic fibers [37].

Fig. 2 shows an example of a cyclic stress–strain curve for a cartilage tissue, wherein there is a large dissipation of energy due to hysteresis in the first few cycles [38]. However, with time, the hysteresis curves almost overlapped. Furthermore, when collagen was removed from the tissue, the tissue showed a mechanical behavior more similar to that of elastin and experienced significantly less stress for the same strain as well as a low dissipation of energy. This elastic behavior under large strains is the main point of focus for the discussion of elasticity in this review.

2.3. Occurrence of elastin in different tissues

Different types of tissues have different mechanical property requirements; some tissues have to be elastic, whereas other tissues have to be stiffer. Therefore, the content and structure of elastin vary within different native tissues. The highest amounts of elastin obtained from the tissue dry weight can be found in elastic ligaments (70%) [2] and large arteries (50%) [2], and the lowest amounts of elastin can be found in the lungs (30%) [2], heart valves (10–15%) [39], skin (2–5%) [40,41], cartilage (1–20%) [42–44], the

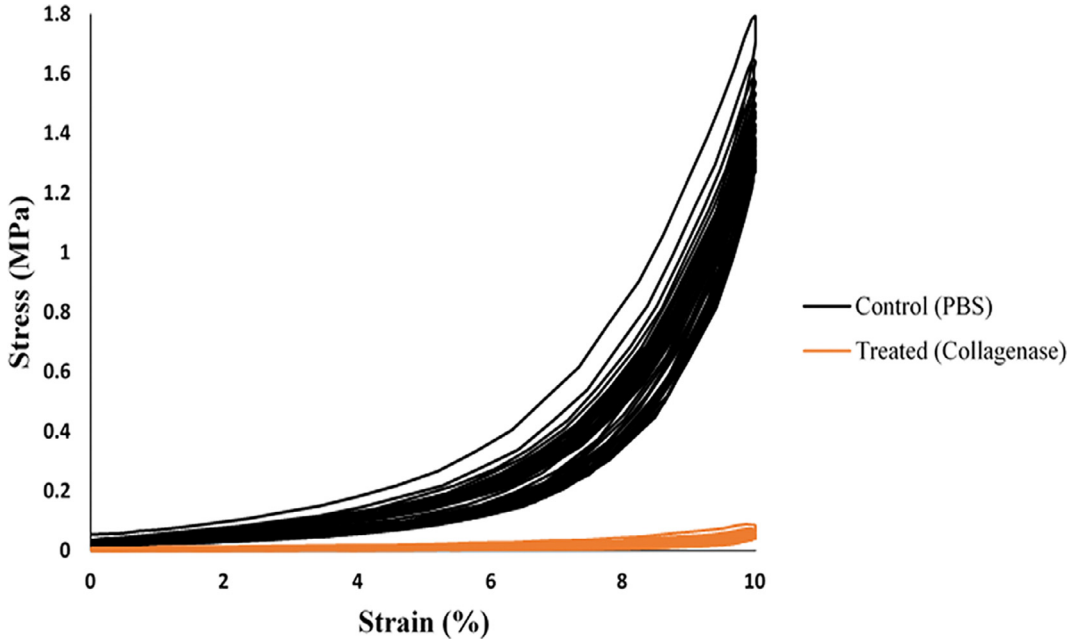

Fig. 2. Stress–strain curves of cyclic compression tests on a cartilage tissue showing the hysteresis loops of a control tissue (black) and a tissue without collagen (orange). As can be seen, the energy dissipation reduced with increase in the number of cycles. Furthermore, removal of collagen led to a lower stress response under the same strain. Reprinted from Fazaeli *et. al.* [38], with permission from Elsevier, copyright 2016. (For interpretation of the references to colour in this figure legend, the reader is referred to the web version of this article.)

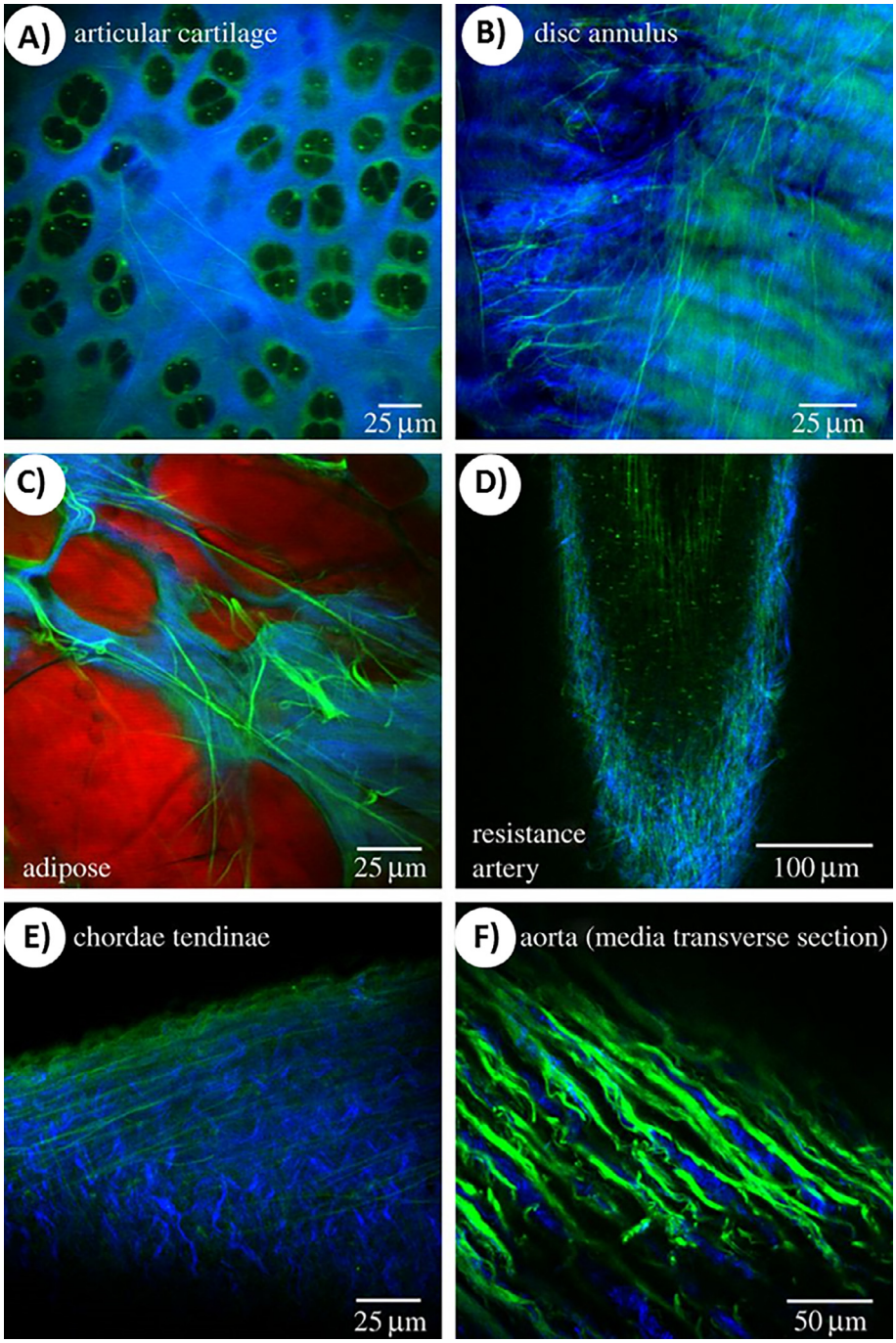

Fig. 3. Visualization of elastin (green) and collagen fibers (blue) showed different structures of elastin for different tissues. A) Articular cartilage from equine metacarpophalangeal joint. B) Intervertebral disc from equine tail. C) Adipose tissue from the human omentum (cells are stained in red). D) Small resistance arteries and veins from human abdominal subcutis. E) Chordae tendinae from porcine heart. F) Porcine aorta. Reprinted from Green *et al.* [37], with permission from the Royal Society, copyright 2014. (For interpretation of the references to colour in this figure legend, the reader is referred to the web version of this article.)

chordae tendineae (2–5%) [45,46], and the intervertebral disc (2%) [47,48], mostly in the nucleus pulposus [37].

Native tissues also differ in the three-dimensional (3D) structure of elastin (Fig. 3). The arrangement of elastin fibers has a tremendous effect on the mechanical behavior of the tissue. In ligaments, arteries, and the skin, elastin mostly forms rope-like structures [2,41], which is then organized in different manners. In ligaments, the fibers show parallel orientations [2] and provide the tissue stress-bearing properties. In elastic arteries such as the aorta, the elastin fibers form concentric lamellae including thick internal and external elastic laminae. This lamellar structure allows the arteries to comply with changes in blood pressure and hemodynamic stresses during the cardiac systole and diastole [49]. On the other hand, in muscular arteries such as femoral arteries, elastin fibers do not form lamellar units [50]. It should be noted that the structure and the amount of elastin in different types of blood vessels depend on their location in the circulatory system because their mechanical properties should match with the local hemodynamic conditions. For example, a comparison between the structure of elastin in cremaster muscle arterioles, which are physiologically subjected to longitudinal stretch, and in cerebral arteries, which are not exposed to longitudinal stretch, revealed

that the longitudinal elastin fibers present in cremaster muscle arterioles were absent in cerebral arteries [51].

The structure of elastin in the cartilage remained unclear for a long time, as elastin was not considered as a crucial component of the ECM owing to its low amount. However, low amounts of elastin can have a large impact on the mechanical properties of the tissue. A study on the articular cartilage showed several microstructures to be present. A fine and dense network of elastin fibers could be found around the chondrocytes. This niche of elastin seems to protect the chondrocytes, as they only experience mild stretching forces even when the cartilage is subjected to relatively larger forces [52]. At the superficial layer, a cobweb-like elastin fiber network could be found. Because it is known that tensile strains are predominantly applied on the surface, the elastin present in this layer could increase the resistance of the cartilage to strain in different directions [52].

Furthermore, in the intervertebral disc, the elastin fibers are organized randomly in their relaxed state. When load is applied, elastin fibers located between the lamellae of collagen fibers form a more organized structure in the extended state than the relaxed state. Herein, the elastin fibers play a role in recoiling the tissue by returning and crimping the collagen fibers to their original preloaded state [57]. Even in low amounts, elastin has an impact on the mechanical properties of the total tissue, particularly by recoiling the collagen fibers after deformation, as observed in the skin [58].

One of the most complex alignments of elastin fibers can be found in heart valves. Heart valves can be divided into three layers, and the elastin fibers are organized differently in each layer. In the fibrosa, elastin forms tubular structures and the fibers are aligned in the circumferential direction [53]. The elastin content in the fibrosa is relatively low, and it is hypothesized that these tubular structures most likely contribute to the stress-tolerance properties of the tissue. However, elastin-rich ventricularis shows elastin fibers arranged in sheets. This structure leads to an extension to up to 60%, which is quite remarkable because collagen is almost inextensible [54]. In the spongiosa, elastin fibers have a sponge-like structure [55]. As the spongiosa functions like a buffer between the ventricularis and the fibrosa, the organization of elastin is to aid this function.

As indicated in the previous section, depending on whether collagen or elastin is the major component of the ECM, the mechanical behaviors of the tissue significantly differ. Thus, when designing a scaffold for a tissue engineering application, it is crucial to define the benchmarks in terms of the amount and particularly the structure of the ECM components, which finally define the mechanical properties of the construct. For example, different layers of the heart valve possess different mechanical properties owing to the different structures and amounts of elastin present in each layer. Consequently, the fracture tension of the elastin fibers in the circumferential and radial directions, respectively, was 0.35 and 0.14 Nm^{-1} for the fibrosa and 2.94 and 2.81 Nm^{-1} for the ventricularis [56]. The structure of elastin and collagen fibers also defines the morphology and alignment of the cells through the contact guidance mechanism, which then influences the alignment of the ECM deposited by the cells.

3. Elastic materials for tissue engineering

As discussed earlier, the elasticity prevailing across numerous deformation cycles of tissue-engineered scaffolds is of importance for the proper functioning of the implants *in vivo*. Because the production of elastin by cells *in vitro* is limited, elasticity has to be introduced into the scaffold material. This section provides an overview of the sources that can be used to gain elastic materials. Additionally, a summary of the mechanical properties of natural materials (Table 1), recombinant materials (Table 2), and synthetic materials (Table 3) and a description of the state of the research for each particular category are provided.

Table 1
List of available elastomeric scaffolds from natural materials for tissue engineering applications (E = Young's modulus).

Category	Material	Material properties	Application	Major outcome
Decellularized tissue	Decellularized bovine arteries [59]	Strain at break Axial = ~150% Circumferential = ~50% Burst strength = 1300 MPa	Blood vessel regeneration	Native architecture was maintained; human saphenous vein endothelial cells adhered to the matrix and formed a monolayer
	Decellularized lungs [66,67]	–	Lung transplantation	Mechanical functionality similar to that of native lungs. Participation in gas exchange was observed in short-term *in vivo* studies (45–120 min)
	Decellularized bladder [68]	–	Bladder regeneration	Long-term *in vivo* studies (22 weeks) showed limited cellular repopulation in the middle of the scaffold. After 22 weeks, no difference was observed in the rupture stress, but a significant decrease was shown for rupture strain. The tissue modulus increased as well
	Decellularized bovine cornea [69]	Ultimate tensile strength = ~3.5 MPa Tissue extensibility = ~6.6	Cornea regeneration	No significant difference in ultimate tensile strength compared to the native tissue. *In vivo* studies showed good biocompatibility
Native elastin	Purified elastin fibers [60]	–	Tissue engineering	Pure and intact elastin fibers showed a significantly lower cell response than partially purified fibers or partially degraded fibers after *in vivo* implantation, which is probably caused by a lower inflammatory response
	Insoluble elastin–collagen [72]	E (wet) = ~3 MPa Yield strain = ~45% Yield stress = ~0.25 MPa	Vascular grafts	Decrease in Young's modulus and yield strain after elastin incorporation into the collagen scaffold as well as an increase in the mature smooth muscle cell fraction
	Soluble elastin-collagen [72]	E (wet) = ~2 MPa Yield strain = ~50% Yield stress = ~0.15 MPa	Vascular grafts	Decrease in Young's modulus and yield strain after elastin incorporation into the collagen scaffold as well as an increase in the mature smooth muscle cell fraction
	Electrospun α-elastin [74]	Tensile strength = 1.6 MPa Ultimate elongation = 0.01	Tissue engineering	Scaffold could support the attachment and growth of human embryonic palatal mesenchymal cells during *in vitro* studies

Table 2
List of available elastomeric scaffolds from recombinant techniques for tissue engineering applications (E = Young's modulus).

Category	Material	Material properties	Application	Major outcome
Tropoelastin	Cross-linked tropoelastin hydrogel [81]	E = 220–280 kPa Elastic until strain reaches 150% Elongation at break = 200–370%	Tissue engineering	Highly extensible gels with elastic behavior up to 150% elongation. *In vitro* studies showed both growth and proliferation, whereas *in vivo* studies showed that the scaffolds were well tolerated
	Tropoelastin-silk [82]	–	Nerve guidance	The growth of both peripheral neurons and Schwann cells was supported by the scaffold
Elastin-like polypeptides	ELP-solution [88]	Shear modulus = 0.15–0.50 Pa	Cartilaginous tissue repair	A threefold increase in shear modulus of the ELP solution at above compared to below the transition temperature. *In vitro* cell studies showed that chondrocytes maintained their phenotype
	In situ cross-linked ELP [90]	Shear modulus = 0.26 kPa	Cartilaginous tissue repair	Mechanical integrity increased *in vivo*, thus suggesting that the original matrix is restructured by the deposition of the functional ECM
	Photo cross-linked ELP hydrogel [91]	E = 1.2–2.2 kPa Ultimate tensile strength = 6.5–10 kPa Extensibility = 3.5–4 Compressive modulus = 3–15 kPa Energy loss under cyclic compression after 8 cycles = 35–50%	Hemostatic material	Mechanical properties could be tuned by changing the concentration. After subcutaneous implantation, long-term structural stability was observed
	Cross-linked ELP gel [92]	E = 0.10–0.32 MPa Shear modulus = 0.04–0.12 MPa Elongation at break = 250–400%	Vascular tissue engineering	Mechanical tests under physiological conditions showed dependence on the cross-linking density

Table 3
List of available synthetic elastomeric scaffolds for tissue engineering applications (E = Young's modulus).

Material	Material properties	Application	Major outcome	Chemical structure
PGS tubes [102]	–	Nerve guidance	Compared to currently used PLGA scaffolds, less inflammation and fibrosis were observed after *in vivo* implantation	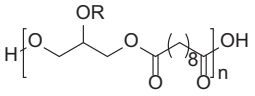
Microfabricated layers of PGS [104]	E = 1.66 MPa Strain at break = 113%	Retina regeneration	Significant improvement of the mechanical properties compared to previous systems. Cell culture showed a tendency towards differentiation necessary for the application	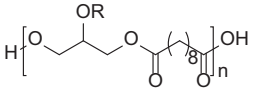
Porous PGS [105,107]	Effective stiffness = 0.83 MPa	Skin and heart valve regeneration	Scaffolds for heart valves showed similar mechanical properties compared to bovine aortic heart valves. *In vitro* cell studies with mouse dermal fibroblasts showed good attachment and proliferation	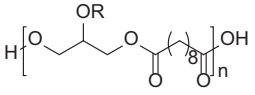
PGS-nanosilicate [106]	Compressive modulus = 28–130 kPa Recovery after 8 compression cycles = 98–99%	Bone tissue engineering	Tunable and promising material properties for bone engineering. *In vivo* studies showed good biocompatibility as well as biodegradability of the scaffold	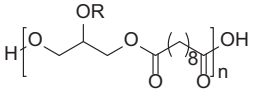
PCL-based PU [114]	Compression modulus = 22.6 kPa (with cells)	Cartilage tissue engineering	Cell attachment and cell proliferation were observed. However, dedifferentiation of chondrocytes and the diffusion of significant amounts of ECM into the media were also observed during 42 days of *in vitro* studies	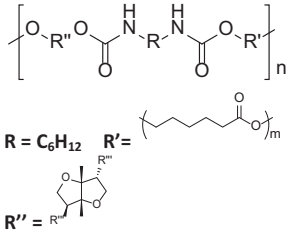

Table 3 (*continued*)

Material	Material properties	Application	Major outcome	Chemical structure
Poly(ester urethane) based on PCL [115]	E = 10 MPa Ultimate tensile stress = 3.3 MPa Strain at ultimate tensile stress = 693%	Myocardial tissue engineering	Promising mechanical functionality for myocardial tissue engineering. Cell studies showed good cell attachment but no proliferation	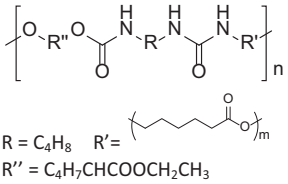
PHA-PLA-PGS [123]	–	Myocardial tissue engineering	Mesenchymal stem cells were properly aligned on the scaffolds and were able to function accordingly	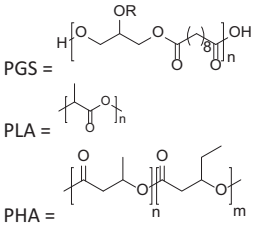
P4HB-GelMA [124]	E = 5.68 MPa Ultimate tensile stress = 2.68 MPa	Pulmonary arterial patch	A functional arterial patch capable of withstanding the physiological conditions upon *in vivo* implantation was fabricated	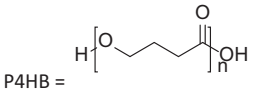
PHB [125,189]	–	Nerve regeneration	*In vivo* transplantation of Schwann cells using PHB conduits showed sustained axonal regeneration	–
PHBHHx [121]	–	Nerve conduit and cardiovascular regeneration	Less platelet adhesion compared to PHB films. *In vivo* studies for nerve conduits showed PHBHHx to be highly compatible; it was also able to form a bridge of the regenerated nervous tissue within 1 month	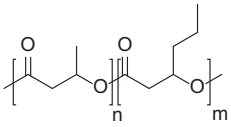
PCL springs [129]	Strain at break = 260%	Cardiac tissue regeneration	Spring-like fibers showed a stronger contraction force and a higher beating rate than straight fibers, thus showing improved qualities for cardiac tissue engineering	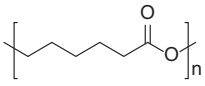
POC [109]	–	Vascular tissue engineering	Good hemocompatibility	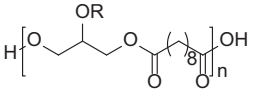
POC-PLLA [110]	Tensile strength = 1.51 MPa Young's modulus = 17.73 MPa Elongation at break = 182% Permanent deformation after tensile failure = 1.88%	Cartilage, ligament, and vascular tissue engineering	Tunable mechanical functionalities suitable for a wide range of tissue engineering applications	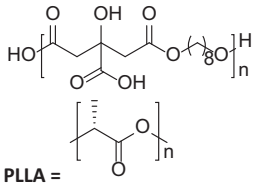

3.1. Animal-derived elastin

Obtaining elastin from the natural ECM that can be used for tissue engineering applications is highly challenging. Different forms of elastin that can be obtained from animal sources are tissues containing elastin [59], purified elastin fibers [60], hydrolyzed elastin [61], and tropoelastin [62]. Decellularized tissues are a natural elastic matrix in which the cells have been carefully removed to avoid an immunogenic reaction [63]. The tissue can then be either reseeded with cells and cultured before *in vivo* application (Fig. 4A) or implanted as an acellular construct [64]. The most important advantage of the decellularization technique is that the ECM structure of the original tissue is preserved. However, as tuning of the elastin properties can be done, the application by this method is limited because other ECM components are still present, which will prohibit the use of a particular tissue for another tissue replacement.

In one study, decellularizing bovine arteries and subsequent *in vitro* cell reseeding led to the high cell viability *in vitro*, and acellular scaffolds had a significantly lower rejection response *in vivo* than the untreated tissues [65]. Furthermore, mechanical testing of the decellularized tissues confirmed that the mechanical strength was preserved during the decellularization process [59]. Decellularized lungs have also shown to be viable both *in vitro* and *in vivo* [66,67]. Furthermore, decellularized tissues from the bladder [68] and the cornea [69] have been successfully tested for tissue engineering applications. Although these results show a potential for using decellularized scaffolds, the process to obtain

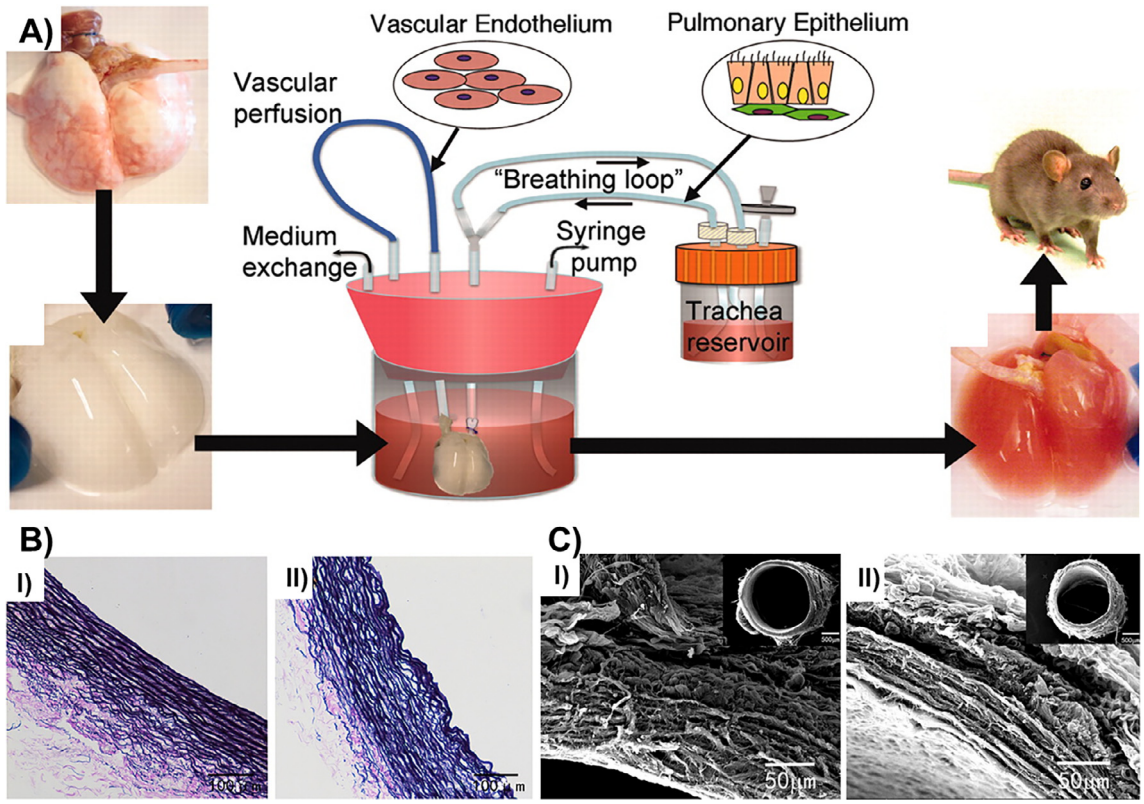

Fig. 4. A) A schematic representation of decellularization procedure of a tissue engineered lung. First, cannulas were made in the lung at the pulmonary artery, and the trachea was filled with decellularization solutions. After 2–3 h, the decellularized tissue was obtained, which is then seeded with pulmonary vascular endothelium using a biomimetic bioreactor. After 4–8 days, the tissue engineered lung was ready for implantation. Reprinted from Petersen *et. al.* [66], with permission from AAAS, copyright 2010. B) Verhoeff-Van Gieson histochemical staining of elastin in native (I) and decellularized (II) tissues showed structural disruption of the fibers. C) Scanning electron microscope images of the cross-section of blood vessels before (I) and after (II) decellularization. Fibers appeared to be rough, and the gap between fibers increased upon decellularization. Reprinted from Gong *et. al.* [71] with permission from Elsevier, copyright 2016.

decellularized tissue changes according to the type of tissue. Furthermore, the use of chemicals and enzymes, in some cases, can influence the mechanical properties of the resulting scaffolds as can be seen in Fig. 4B and 4C. In Fig. 4B, the Verhoeff-Van Gieson staining method was used to stain the native (Fig. 4B, I) and decellularized (Fig. 4B, II) tissues for elastic fibers. As shown in the figure, the structure of the native tissue is disrupted because of decellularization. In addition, in Fig. 4C, scanning electron microscope images of blood vessels in the native (Fig. 4C, I) and decellularized (Fig. 4C, II) tissues show a large distance between the fibers upon decellularization. In Fig. 4C, II, it can be seen that the fibers are disconnected [2,22,70,71]. It should be noted that there is a compromise between removal of all cellular material and preservation of the ECM structure. The feasibility of current decellularization protocols depends on the acceptability of this balance for each application.

Pure elastin fibers can also be obtained from animal sources. Mature elastin, however, is highly insoluble because it is cross-linked, thus making purification and processing of elastin challenging. The main drawback of elastin purification is that it often damages the fibers, especially if all remnants of microfibrillar components are removed. However, Daamen *et al.* optimized the protocol to obtain pure intact elastin fibers [60]. Purified elastin can be fabricated to scaffolds with different structures depending on the target application. However, the structure of decellularized tissues cannot be modified for different target tissues. Incorporation of insoluble elastin into electrochemically aligned collagen (ELAC) fibers led to a decrease in yield stress and Young's modulus (from 10 to 2 MPa) both before and after culturing with smooth muscle cells, whereas the yield strain was comparable, thus showing the influence of elastin incorporation on mechanical properties [72]. In the same study, soluble elastin, prepared by oxalic acid treatment, was incorporated into ELAC fibers, and the resulting mechanical properties were similar to those of insoluble elastin [72]. It should be mentioned that solubilizing the elastin through hydrolyzation of the peptide chains increases the processability.

Hydrolyzation of elastin by different agents results in different elastin fragments. For example, hydrolyzation of elastin by oxalic acid treatment resulted in two different fractions: α-elastin (~60 kDa), which shows the typical reversible coacervation behavior, and β-elastin (~5 kD), which is present in the supernatant at all temperatures [2,61]. Moreover, κ-elastin (~70 kDa) is obtained by hydrolysis with potassium hydroxide [2,14,73]. Different methods based on enzymes can also be employed to obtain soluble elastin, but the resulting elastin fragments differ according to the enzyme used [2,14]. Electrospinning of α-elastin led to brittle scaffolds; however, these tests were performed under dry conditions wherein elastin does not exhibit elastic behavior. Furthermore, the scaffold could not support cell attachment, migration, and proliferation [74]. This result is counterintuitive with the advantage of natural materials, which usually provide a better biological response than synthetic materials. It is possible that solubilization reduces the biological response. Furthermore, the absence of other ECM components could be the reason that cell studies did not yield desirable results. Although soluble elastins are better to process, hydrolyzation compromises the mechanical properties of the resulting peptides. Additionally, results depend on both the source of elastin and the method used, therefore influencing the reproducibility.

Finally, tropoelastin can be obtained from copper-deficient animals when harvested during the late fetal or early neonatal stage [62]. In this stage, crosslinking is prevented because copper is an essential cofactor for the crosslinking enzyme lysyl oxidase [75]. However, the single tropoelastin moieties are prone to degradation by proteases because of free amine moieties [76]. If tropoelastin extraction is successful, then it results in molecules with various molecular weights [77]. All the above-described methods have the disadvantage of using animals as a source, thus leading large batch-to-batch variations and also difficult processability of materials. Furthermore, tuning of such materials and thus their properties is limited. Therefore, materials with easy processability and tunable chemical and mechanical properties are favorable for application.

3.2. Elastin production by recombinant techniques

Recombinant techniques, mostly using bacteria, provide controllable and well-defined results for protein synthesis. The first report on the expression of the complete tropoelastin molecule in a bacterial system (*Escherichia coli*) was published in 1990 [78]. The tropoelastin molecule produced by recombinant techniques is obtained as single strands. Further processing of this tropoelastin molecule with lysyl oxidase yields insoluble elastin, even in the absence of other macromolecules. However, the location of the crosslinks between the synthetic elastin molecules and the alignment of the synthetic elastin fibers will not be same as those in native mature elastin without the guidance of the other macromolecules [79]. Further investigation showed that recombinant tropoelastin could be incorporated into the ECM by non-elastogenic rat-1 fibroblasts that express lysyl oxidase [80].

Tropoelastin can be used for many tissue engineering applications; for example, it can be used as a chemically cross-linked hydrogel [81]. The scaffold produced this way had a Young's modulus of 220–280 kPa and showed elastic behavior until an extension of 150%, with the final extension at a break of 200–370% [81], thereby making it an interesting material for tissue engineering of elastic tissues. Moreover, blending of tropoelastin and silk produced a material that improved cell growth and was used for nerve guidance [82]. Tropoelastin has recently been used in many studies because it not only can serve as an elastic component with biological recognition in the scaffold material but also is a potential elastogenic molecule that can stimulate the synthesis of elastin.

By changing the genetic code on the vector incorporated in the bacteria, proteins that are different from those available in nature can be produced, which remarkably increases the possibilities. For example, a polypentapeptide, $(VPGVG)_n$, derived from the repeating pentapeptide in elastin was synthesized in bacteria in 1974 [83]. Interestingly, this polypentapeptide showed coacervation behavior in region same as that of α-elastin obtained from the pig aorta [83]. Inspired by these results, more changes were made in the amino acid sequence, thus leading to elastin-like polypeptides (ELPs). The amino acid sequence of the ELPs was on the basis of the sequence VPGXG, where X is any amino acid except proline [84]. These ELPs also showed coacervation behavior upon increasing the temperature. The transition temperature of these ELP solutions could be influenced by the length of the peptides, the amino acid residues at position X, and external stimuli such as salt concentration and pH [85,86]. Furthermore, these ELPs have been shown to be highly biocompatible [87], therefore making it an interesting candidate for tissue-engineered scaffolds.

Several successful scaffolds based on the ELPs were made for engineering cartilage tissues. One is the ELP solution with viscoelastic properties, which was proposed to be used as an injectable scaffold in the future [88]. However, this is based on single strands of the ELP that cannot withstand the load applied to the cartilage *in vivo*. *In situ* cross-linking of ELP gels yielded positive results to overcome this in a goat osteochondral defect model [89]. The crosslinking increased the dynamic shear stiffness of the material from 0.08 to 0.26 kPa, and after culturing with cells for 6 days, the stiffness further increased to 1.7 kPa [90].

ELP hydrogels could be modified to be photo cross-linked. Cysteine moieties introduced at both the C- and the N-terminus of the peptides can be cross-linked using a photoinitiator and a reducing agent [91]. The photo cross-linkable hydrogels showed good mechanical properties [91]. Fig. 5A shows high extensibility of the 10% w/v ELP hydrogel up to 310%, and Fig. 5B shows the stress–strain curves of this material under cyclic compression, thus showing the elasticity of the material. Furthermore, *in vivo* testing showed early ingrowth of the noninflammatory tissue into the ELP gel, showing biocompatibility and integration of the ELP hydrogel (Fig. 5C). These functionalities make the ELP hydrogel particularly promising to be used as a sealant for soft tissue injuries [91]. Different cross-linked ELP gels with Young's moduli of 100–300 kPa have also been investigated for vascular graft applications [92,93].

3.3. Synthetic elastomers

A completely different approach is using synthetic elastomers in tissue engineering applications. These materials have no structural link to elastin but can still exhibit the same mechanical functionality. Scaffolds based on synthetic elastomers have the advantage that they can be easily modified at both small and large scales [9] by either chemical alteration of the polymeric chain, for example, by changing the monomer [94], or by postmodifications, for example, by crosslinking [95]. Furthermore, they can be molded into virtually any shape and size [96]. Therefore, synthetic elastomers are widely investigated for tissue engineering applications. Although many synthetic elastomers show potential characteristics for tissue engineering applications [96], they have not all been tested for their feasibility with regard to this. Herein, only the synthetic elastomers that have already been investigated for tissue engineering purposes are discussed. This review does not include polymers that are not classified as elastomers, such as poly(lactic acid) (PLA) [97–99] or poly(ethylene glycol) (PEG) [100,101].

Poly(glycerol-*co*-sebacate) (PGS) is a polyester elastomer investigated for a range of different applications within the field of tissue engineering. Tubes made of PGS are excellent candidates for biodegradable peripheral nerve repair, especially because they do not swell in water [96,102,103]. A scaffold can be prepared for retina regeneration by processing PGS so that it forms microfabricated layers on which retinal progenitor cells can be seeded [104]. Furthermore, porous PGS scaffolds, processed by laser ablation, could mimic the peak tangent moduli (maximum slope of the stress–strain curve) of bovine aortic heart valves in both circumferential (PGS scaffold, 0.83 MPa; Native heart valve, 1.00 MPa) and radial directions (PGS scaffold, 0.21 MPa; Native heart valve, 0.26 MPa) [105].

Recent studies have also indicated that PGS in combination with nanosilicates is a promising candidate for bone tissue engineering [106]. The combination of elasticity and tunable stiffness was particularly favorable to provide the scaffold the ability to withstand the loading and influence the regeneration of the bone. Furthermore, the nanosilicates enhanced the growth rate of bone cells. The porous structure of the scaffolds became more rough with an increasing amount of nanosilicates (Fig. 6A), which might enhance cell adhesion and spreading [106]. The biocompatibility was tested *in vivo* in mice, the results showed infiltration of cells into the scaffold after 3 and 6 days (Fig. 6B). Moreover, different porous scaffolds made of PGS and fabricated through leaching techniques have been used for skin regeneration [107]. Although PGS scaffolds show favorable mechanical functionalities, they lack motifs to stimulate cell adhesion. Thus, surface modification techniques

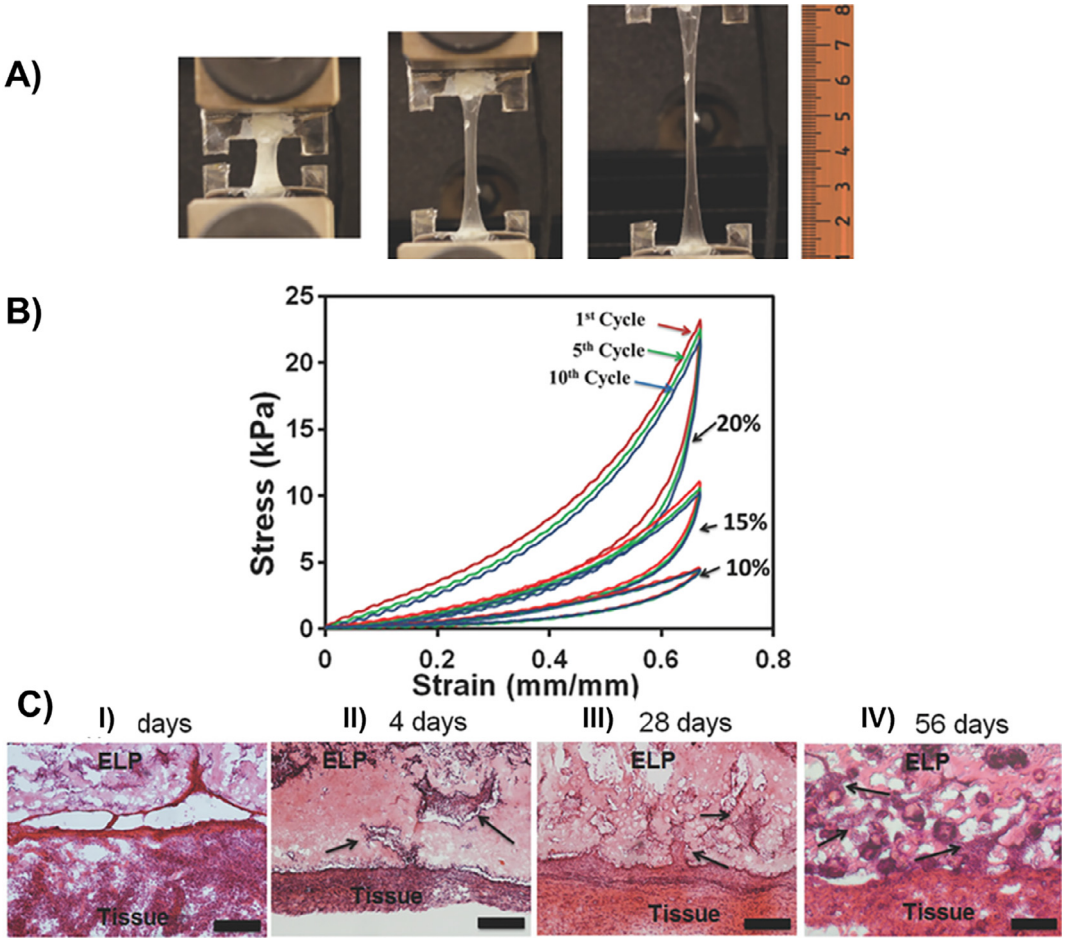

Fig. 5. Highly elastic cross-linked ELP hydrogels. A) Photographs of the ELP hydrogel under 0% (left), 260% (middle), and 310% (right) strain. B) Cyclic loading and unloading of the hydrogels under compression tests. C) *In vivo* tests showed early integration of the ELP hydrogel by non-inflammatory tissue. Reprinted from Zhang *et. al.* [91] with permission from John Wiley and Sons, copyright 2015.

have to be employed to promote cell adhesion (Fig. 6C) [108]. For example, in this case, an RGD motif was introduced onto a PGS polymer, which is known to promote cell adhesion.

A different type of polyester elastomers is poly(diol citrate). Poly(1,8-octanediol-*co*-citrate) (POC) is often used for tissue engineering purposes. POC-based films were compared with hemocompatible FDA-approved materials to evaluate their feasibility for vascular tissue engineering. Hemocompatibility tests showed low attachment of platelets and low protein binding and that the endothelial cells retained their morphology under flow conditions, thus showing encouraging results [109]. POC was also mixed with a poly(L-lactic acid) (PLLA) nanofiber network to provide reinforcement to the scaffold. Mechanical properties of these scaffolds were analyzed, and the material was hypothesized to be feasible for use for ligament, vascular, and cartilage tissue engineering; however, neither *in vitro* nor *in vivo* testing has been carried out yet [110].

Another class of synthetic elastomers is polyurethanes (PUs). This large class of elastomers varies in chemical structure, mechanical functionality, and also degradation profile and has therefore often been studied for various tissue engineering applications [111,112]. A PU based on lactic acid urethane and maleate was investigated for bone tissue engineering as load-bearing bone fillers [113]. Young's moduli of this PU material were measured under compression, tension, bending, and torsion. The results showed similar or even better mechanical properties than previously designed bone fillers. Furthermore, cell seeding with human bone marrow and endothelial cells showed rapid cell attachment and high biocompatibility with both cell types [113]. However, these materials are not as strong as native bone and can therefore only be used in a period of recovery in combination with fixation of the bone and minimized physical load.

Different PUs have also been investigated for cartilage tissue regeneration [114]. Attachment of chondrocytes to these scaffolds, as well as their growth and differentiation, was supported to up to 42 days *in vitro* [114]. In addition, production of ECM components was observed. However, dedifferentiation occurred after prolonged culturing. The authors proposed that mechanical loading might prevent dedifferentiation of the cells and trigger the formation of a functional cartilage mimic. Cardiac patches for myocardial tissue engineering have also been fabricated using PUs [115]. In this case, a bilayer scaffold based on a poly(ester urethane) synthesized with poly(ε-caprolactone) (PCL) diol, 1,4-butanediisocyanate, and L-lysine ethyl ester dihydrochloride was fabricated. The mechanical functionality tests showed a Young's modulus of approximately 10 MPa with an ultimate tensile stress of 33 MPa. Cyclic tensile tests were performed to up to 10% deformation, where the stress response increased only 3.1% across the cycles, and the material showed elastic behavior in that region [115]. Other applications for PU-based scaffolds are in the fields of nerve regeneration [112] and heart valve tissue engineering [9]. Not only the potential applications of PUs in tissue engineering were investigated, continued research has also been conducted in inventing new ways to design scaffolds [116,117] and in understanding and tuning the degradation of these scaffolds [111,118].

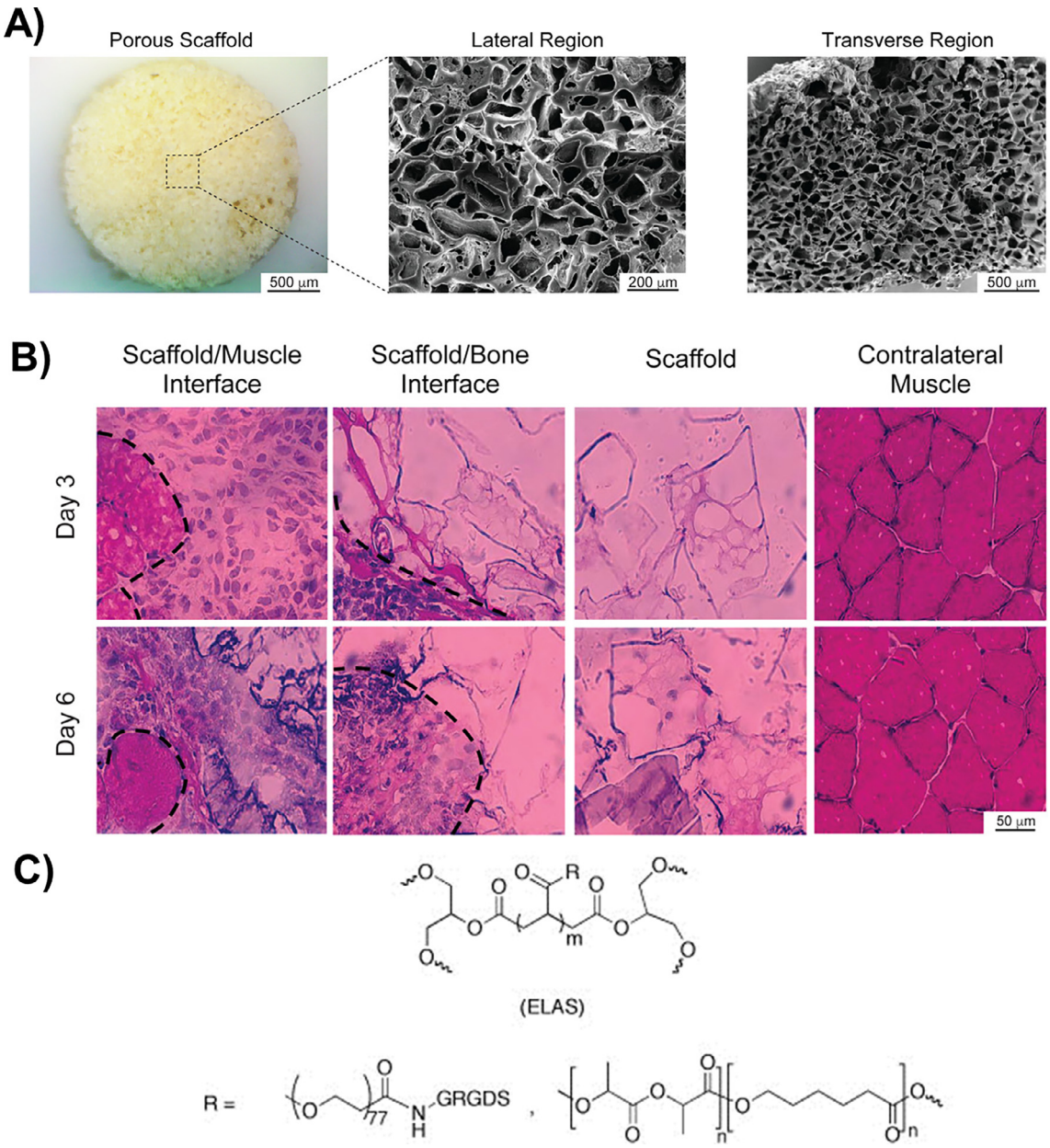

Fig. 6. A) Histological analysis showed cell infiltration into the scaffold after 3–6 days of implantation. Scaffolds were implanted between the quadriceps and the femur bone in mice. B) General overview of the porous structure of PGS-nanosilicate materials with detailed representation of the lateral/exterior region and the lateral/transverse cross-section. Reprinted from Kerativitayanan *et. al.* [106], with permission from ACS publications, Copyright 2017. C) An example of the PGS polymer functionalized with PEG-Gly-Arg-Gly-Asp-Ser(GRGDS) modification to enhance cell adhesion. Reprinted from Ilagan and Amsden [108], with permission from Elsevier, copyright 2009.

Depending on the monomer composition, poly(hydroxyalkanoate)s (PHAs) can have an elastic nature; for example, medium-chain length PHAs show elastic behavior [119] and have therefore been used in a range of biomedical applications [120]. Poly(4-hydroxybutyrate) (P4HB) is a type of PHA used in cardiovascular applications. The degradation of pure P4HB is quite fast [121], thus making it unfavorable for cardiovascular applications that usually need longer mechanical functionality of the scaffold. However, P4HB can be used for coating scaffolds such as poly(glycolic acid) to provide initial mechanical integrity before the cells produce their own ECM [122]. It has been shown that by electrospinning a blend of a type of PHA with poly(L-D,L-lactic acid) and PGS, a thick myocardial patch could be produced [123].

Recently, a combination of P4HB and methacrylated gelatin (GelMA) resulted in a scaffold that was successfully implanted as a pulmonary arterial patch [124]. In this case, the fibrous structure of P4HB was surrounded by a hydrogel made of photo cross-linkable methacrylated gelatin. This patch was implanted into a sheep model where it showed no thrombogenicity and could withstand the physiological loading conditions. Furthermore, within cylindrical scaffolds of poly(3-hydroxybutyrate) (PHB), nerve regeneration was observed within 1 month in both myelinated axons and Schwann cells [125]. A more recently developed PHA, called poly(3-hydroxybutyrate-*co*-3-hydroxyhexanoate) (PHBHHx) [121], was found to be less brittle and showed better biocompatibility than the previously reported PHA polymers. Applications of this polymer in tissue engineering are quite broad owing to the tunable mechanical properties. Thus far, its use has been reported for bone, cartilage, nerve, brain, smooth muscle, and soft tissue engineering [126,127].

A different polymer that is a potential candidate for tissue engineering applications is PCL [128]. For example, PCL was used to mimic the 3D structure of cardiac tissues by synthesizing spring-like PCL fibers by changing the speed of electrospinning from 7 ml/h for straight fiber to 0.5 ml/h for spring-like fibers [129]. The rationale behind producing spring-like PCL fibers comes from the structure of native cardiac tissues, where straightening and recoiling of these fibers make the muscles contract in the direction of the cardiomyocytes [130]. These spring-like fibers were compared with the straight PCL fibers in a test with single cardiomyocytes, and it was shown that the contractions of cardiomyocytes could not contract the straight fibers but could move the spring-like fibers in a repetitive manner. The spring-like fibers showed a lower Young's modulus and a higher strain at failure than the straight ones. Well-defined structures with a range of mechanical properties can be produced using PCL, thus increasing its potential for tissue engineering applications [131].

For many tissue engineering applications, combinations of different materials are made to obtain the proper mechanical functionalities necessary to create a particular functional tissue. In the cases explained thus far, noncovalent mixtures of materials have been used. However, improvement in the mechanical and biological properties can also be made by using covalent links between different materials such as two different proteins or protein derivatives, two synthetic polymers, or a combination of these two classes. The possibilities of these material combinations in the field of tissue engineering are reviewed in the next section.

4. Elastic hybrid materials for tissue engineering

The rationale behind preparing hybrid materials instead of using single-component materials is to combine the positive functionalities of each material to create a construct that has better overall properties such as mechanical functionality, biocompatibility, and (bio)degradability. For example, materials with good mechanical properties that lack motifs for cell attachment or proliferation could be combined with proteins or polymers that can enhance these properties. Such combinations lead to a material with easier processability and smaller batch-to-batch variations than a material containing only proteins for instance. Examples of the materials with the above-mentioned enhanced properties can be found in the following sections. Although these advantages can lead to the use of better performing materials for tissue engineering constructs, synthesizing hybrid materials can be highly challenging, especially when different fabrication techniques have to be employed. Therefore, a balance between the complexity of the production and fabrication processes and the benefits present in hybrid materials has to be maintained.

In this section, hybrid materials are classified into three different categories, namely, polymer–polymer, protein–protein, and polymer–protein hybrids. Notably, hybrid materials are considered to have a covalent crosslink between their different components. In addition, an overview of the synthetic polymer–synthetic polymer hybrids (Table 4), protein–protein hybrids (Table 5), and synthetic polymer–protein hybrids (Table 6) is given, and the available mechanical data and the major outcomes of the research for each material are shown.

4.1. Synthetic polymer–synthetic polymer hybrid materials

Different polymers provide different characteristics. Whereas some materials such as poly(lactic-*co*-glycolic acid) (PLGA) can be easily degraded [132], other materials such as PGS have more favorable mechanical functionalities like elasticity [9]. Often, a combination of these properties is necessary to obtain the desired properties for tissue-engineered scaffolds.

Improving mechanical functionalities is a major reason for combining polymers. For example, PLGA is a good candidate for tissue engineering with high biocompatibility and biodegradable properties; however, this material can be quite brittle [133]. Therefore, a copolymer of poly(glycolide-*co*-ε-caprolactone) (PGCL) was synthesized, and it showed a high increase in elastic behavior compared to PLGA [133]. Some examinations of rat smooth muscle cells cultured on PGCL showed adhesion of the cells after 3 days, and seeded PGCL scaffolds implanted subcutaneously in mice showed smooth muscle tissue formation *in vivo* [133]. Introduction of ε-caprolactone (CL) into poly(1,3-trimethylene carbonate) (PTMC) resulted in a decrease in crystallinity of the scaffold compared to PTMC [134], thus making poly(TMC-*co*-CL) a suitable scaffold for nerve guidance. The human Schwann cells cultured on the poly(TMC-*co*-CL) scaffold showed good adhesion and a proliferation rate similar to that of human Schwann cells cultured on gelatin, which was used as a positive control [135].

In another study, to obtain an elastic hydrogel, PEG crosslinks were introduced between polyacrylamides (PAs) and poly(acrylic acid) (PAA) [136]. The use of star-shaped PEG polymers with different molecular weights as cross-linkers, instead of linear cross-linkers, greatly improved the extensibility of the material to up to 15000%. Cyclic tensile tests were performed with a maximum strain of 400% [136]. Furthermore, the compression deformation of these hydrogels could be performed to up to 98%, with a limited deformation of the gel. To further analyze the feasibility of using this hydrogel for tissue engineering applications, more studies both *in vitro* and *in vivo* have to be performed. To influence the mechanical properties of poly(glycerol adipate) (PGA), it was copolymerized with ethylene glycol [137]. The amount of ethylene glycol introduced led to a decrease in Young's modulus and an increase in the maximum deformation. Additionally, cell culture studies showed that fibroblasts were differentiated into neuron-like cells [137]. An elastomer was also created by introducing either butadiene or ethylene-butadiene blocks into polystyrene to form poly(styrene–butadienestyrene) (PSBS), known as a thermoplastic elastomer, and poly(styrene-ethylene-butadiene-styrene) (PSEBS) [138]. Introduction of the ethylene-butadiene segment led to better oxidative resistance and more elastic properties than introduction of only butadiene. Both PSBS and PSEBS showed declining hysteresis as the number of cycles increased. However, it was shown that by changing the polymer backbone, the final mechanical properties such as elasticity were influenced [138].

Combining mechanical properties with favorable degradation behavior is vital for tissue engineering materials because the degradation of the implanted scaffold allows for tissue ingrowth and remodeling [139]. PCL exhibits elastic behavior but degrades very slowly, whereas PLGA has a favorable degradation time but is highly brittle on its own [140]. Combining PCL and PLGA into a triblock copolymer therefore resulted in rapidly degradable polymers with elasticity. The degradation time of PTMC, as a highly elastic material, was also sped up by introducing PLA [134]. In another study, copolymerizing TMC and L,D-lactic acid (LDLA) led to amorphous elastomers with tunable degradation [141]. By using a mole ratio of 20% TMC to 80% LDLA, a scaffold was designed for cardiac tissue engineering application, which not only was flexible and stable under physiological conditions but also allowed adhesion and proliferation of cardiomyocytes [142].

To create a material with a slower degradation rate than PGCL, CL was copolymerized with a different lactone, called lactic acid, which resulted in the copolymer poly(L-lactide-*co*-ε-caprolactone) (PLCL). PLCL has gained particular interest for its use in vascular tissue engineering owing to its high elasticity [143,144]. Tubular PLCL scaffolds were prepared by an extrusion-

Table 4
List of available elastomeric hybrid scaffolds consisting of multiple synthetic polymers for tissue engineering applications (E = Young's modulus).

Material	Properties	Application	Major output	Chemical structure
Poly(TMC-*co*-LDLA) (20–80% mole ratio) [142,190]	E = 1900 MPa Maximum strength = 51 MPa	Heart tissue engineering	Suitable mechanical properties and degradation behavior. *In vitro* studies showed adhesion and proliferation of cardiomyocytes	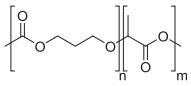
Poly(TMC-*co*-CL) (80–20% mole ratio) [134,135,190]	E = 5 MPa Maximum strength = 2 MPa	Nerve guidance	Suitable mechanical properties; promising *in vitro* studies showed adhesion and growth of human Schwann cells	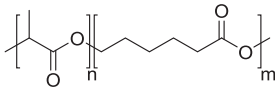
PGCL [133]	Recovery of 98% for strains up to 120% Elongation at break = 250%	Vascular grafts	Mechanical properties showed high recovery; *in vivo* studies showed formation of smooth muscle tissue	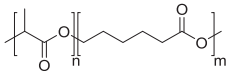
PLCL [144,191]	Deformation at failure after 27 days (10% amplitude and 1 Hz frequency) = 10%	Vascular grafts	Suitable mechanical functionality even for long-term cyclic studies under *in vivo* conditions. Good adhesion and proliferation of smooth muscle cells	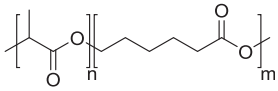
PLCL [145]	Initial modulus = 9.34–24.6 MPa Estimated compliance = 0.052–0.0159 ml*mm/Hg	Vascular grafts	Compliance in the region of natural arteries; slow initial cell proliferation that increased over time	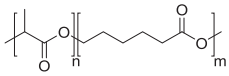
PLCL [148]	E = 0.37–0.73 MPa Elongation at break = 136–520% Recovery = 94%	Cartilage regeneration	The high recovery of the material after loading indicates that the material can be suitable for cartilage regeneration. *In vitro* and *in vivo* studies showed chondrogenic differentiation and mature cartilaginous tissue formation	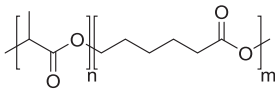
PGLCL [149]	E = 90–140 Pa Maximum strength = 14–38 kPa	–	Mechanical properties similar to those of PLCL and PGCL but with faster degradation and more tunability	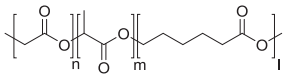
PCL-PDMS [152]	E = 14–32 MPa Tensile strength = 3.8–10.5 MPa Recovery = 91–97%	Bone tissue engineering	Shape memory polymer showing proliferation of human fetal osteoblasts *in vitro* as well as early bone matrix formation	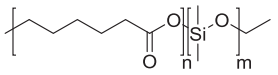
PLGA-PCL-PLGA [140]	E = 20–26 MPa Elongation at break = 400–480%	–	Rapidly degradable and elastic polymer	PLGA PCL 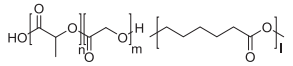
PCL-PIBMD [153]	at 25 °C: E = 200 MPa Elongation at break = 680% at 75 °C: E = 30 MPa Elongation at break = 70% Recovery = 97%	Soft tissue engineering	Shape memory material; *in vitro* testing showed good cell viability and increased cell activity	PIBMD,PCL 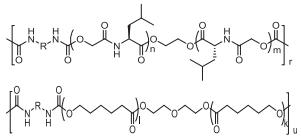
PSBS [138]	E = 0.03–0.23 MPa Elongation at break = 333–442%	–	No cell toxicity was observed after 72 h	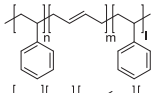
PSEBS [138]	E = 9–38 MPa Elongation at break = 585–1173%	–	Higher elongation at break than PSBS, and no cell toxicity was observed after 72 h	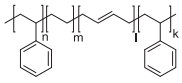
PEGS-AP [150]	E = 15–25 MPa Elongation at break = 50–1113% Fatigue free in cyclic tensile tests after the first cycle	Skeletal muscle tissue engineering	Conducting an elastomeric scaffold that not only allowed proliferation of cells, but also showed to promote cell differentiation for C2C12 cells	PEGS, analine pentamer 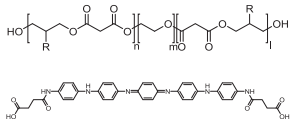
PEG-PA or PAA [136]	Elongation at break = 12,000–15,000%	–	Highly extensible hydrogel with sufficient strength and good recovery	PEG PA PAA 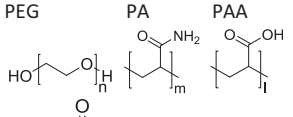
PGA-PEG [137]	E = 0.07–1.18 MPa Ultimate tension = 0.16–0.35 MPa Ultimate deformation = 30–200%	Soft tissue engineering applications	Ethylene glycol allowed for tunable mechanical functionality. No cytotoxicity and good adherence of cells; fibroblasts showed differentiation toward neuron-like cells	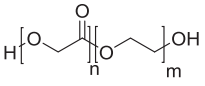

particulate leaching technique and were characterized by cyclic tensile strain tests in the culture media with amplitude and frequency similar to those applied to vascular smooth muscle tissues *in vivo* [144]. Tubular structures of the same material were also fabricated by melt-spinning or electrospinning methods [145]. In this study, a comparison between the mechanical properties of the obtained scaffolds and natural arteries revealed that peak stress and strain values of the scaffolds were higher than those of natural arteries, but the compliance had a magnitude same as that of natural arteries. Cell proliferation on these scaffolds was initially slow but increased with progression of time [145]. Recently, more changes were made in the production method, thus leading

Table 5
List of available elastomeric protein–protein hybrid scaffolds for tissue engineering applications (E = Young's modulus).

Material	Properties	Application	Major output
Elastin-collagen [154]	E = 0.42–0.78 MPa Tensile strength = 142–420 kPa	Tissue engineering	*In vitro* tests with fibroblasts and myoblasts showed positive results. However, no target tissue for the final application has been defined
Elastin-collagen [155]	E = 2.0–8.3 MPa Yield stress = 0.06–0.26 MPa Yield strain = 15–35%	Small-diameter blood vessel regeneration	Cyclic tests have only been carried out on noncross-linked material. *In vitro* studies with smooth muscle cells for 14 days showed cells on both the surface and inside of the 3D scaffolds
Tropoelastin-collagen [156]	E = 166–841 kPa	Dermal tissue engineering	*In vitro* and *in vivo* studies showed fibroblast proliferation, collagen synthesis, and blood vessel formation within the scaffold
ELP-collagen [157]	Shear modulus increased with increasing ELP content	Wound dressing and vascular tissue engineering	Different cell lines were tested for their compatibility; a reduction in the activity of fibroblasts was observed but no changes for endothelial and smooth muscle cells were observed compared to those for collagen
Silk fibroin-elastin [158]	–	Wound dressing	Wound healing studies showed increased keratinocyte and fibroblast migration as well as coverage of the wound with the new epithelium tissue
Silk-tropoelastin [159]	E = 26–54 MPa Elongation at break = 25–56%	Neuronal tissue engineering	Increasing the tropoelastin amount in the scaffold allowed for more adhesion of neurons to the surface
SELP [160]	E = 1.67–3.34 MPa Viscoelastic behavior up to 40% strain Resilience = 86–88%	–	A material with elastic properties similar to those of the native aortic elastin was obtained
Electrospun SELP [163]	E = 142 MPa Ultimate tensile strength = 14 MPa Strain to failure = 22%	Tissue engineering	Good mechanical properties in combination with good viability and proliferation of human skin fibroblasts

Table 6
List of available elastomeric synthetic polymer–protein hybrid scaffolds for tissue engineering applications (E = Young's modulus).

Material	Properties	Application	Major output	Synthetic part of the structure
PEG-AKELP [164,165]	E = 0.32 MPa (dry)/0.12 MPa (hydrated)	Tissue engineering	Indirect cytotoxicity tests showed results same as those of the control; however, direct cell studies showed low adhesion, which was improved by introducing an RGD motif	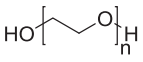
PEG-ELP [166]	E = 2.5 kPa	Tissue engineering	Addition of PEG increased the transition temperature compared to pure ELP. Additionally, it lowered the E value. Cell studies showed a cell viability of 98% after 4 and 7 days	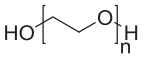
PNPHO-elastin [167]	Compression modulus = 40–150 kPa	Injectable hydrogel	Mostly focusing on tuning the gelation temperature. Cell viability was above 80% when encapsulated	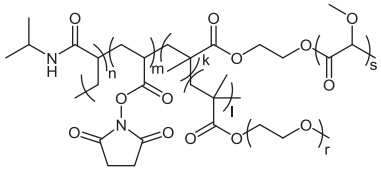
PLGA-elastin [168]	E = 20.78 MPa	Salivary epithelial cell self-organization	Cross-linked PLGA fibers connected to elastin. Lower cell integration into the scaffold than the non-cross-linked PLGA scaffold, probably because of crosslinking	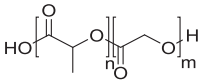
Hyaluronan-PEGDA-ELP [169]	Mean initial aggregate modulus = 17–32 kPa Mean peak stress at 10% strain = 67–79 kPa Mean peak stress at 40% strain = 179–200 kPa	Nucleus pulposus of the intervertebral disc	Cyclic compression tests under 10% and 40% strain Decrease in cell viability after 3 weeks in the *in vitro* tests with the disc	Hyaluronan, PEGDA 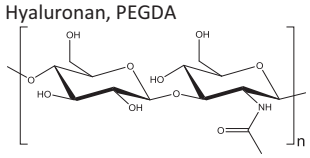 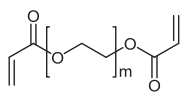

to better functioning scaffolds that showed, for instance, a higher burst pressure [146,147]. PLCL has also been investigated for cartilage tissue regeneration, and the formation of mature cartilage tissue was shown *in vivo* [148]. To obtain a better control of the degradation rate of PLCL-based scaffolds, the polymer was modified using two different lactones, thereby resulting in poly (glycolide-*co*-L-lactide-*co*-ε-caprolactone) (PGLCL) [149]. Although mechanical properties and cell viability of PGLCL were similar to those of PLCL and PGCL, the degradation rate increased [149].

To provide proper functionality to some tissue engineering scaffolds, a combination of more than two materials is needed. For example, three different characteristics were combined in a copolymer of PEG, PGS, and aniline pentapeptides (APs) [150]. Polyanilines are well-known polymers with tunable conductivity that could be used to introduce an electrical stimulus, known to have a positive effect on the development of functional cardiac and skeletal muscle tissues. However, these materials are difficult to process. To improve the mechanical functionality, elastic PGS is used, but PGS is slowly degradable and has poor water uptake. It is known that the copolymerization of PEG and PGS resulting in PEGS leads to elastic hydrogels with tunable degradation [150]. Combining PEGS with AP and subsequent crosslinking with hexamethylene diisocyanate (HDI) resulted in elastomeric and conductive films (Fig. 7A). It was shown that increasing the AP concentration increased the elasticity of the scaffold. Cyclic tensile tests, performed for 10 cycles, showed a large hysteresis for the first loop (Fig. 7B). This is probably attributed to π-π interactions between the AP fragments present before the first cycle, which are not regained in the cyclic process. The cycles overlap after the first one, thus leading to the inclination that a fatigue-free material might have been obtained. These materials are particularly useful for skeletal muscle tissue engineering because the conducting polymers are shown to promote myogenic cell differentiation of C2C12 cells (Fig. 7C) [150].

Shape memory materials are favorable in tissue engineering because they allow for noninvasive implantation surgery owing to the fact that they can be transplanted using small catheters. Once implanted, they will expand and gain their final structure [151]. To obtain an elastic material with the shape memory effect, CL was copolymerized with dimethyl siloxane into PCL-

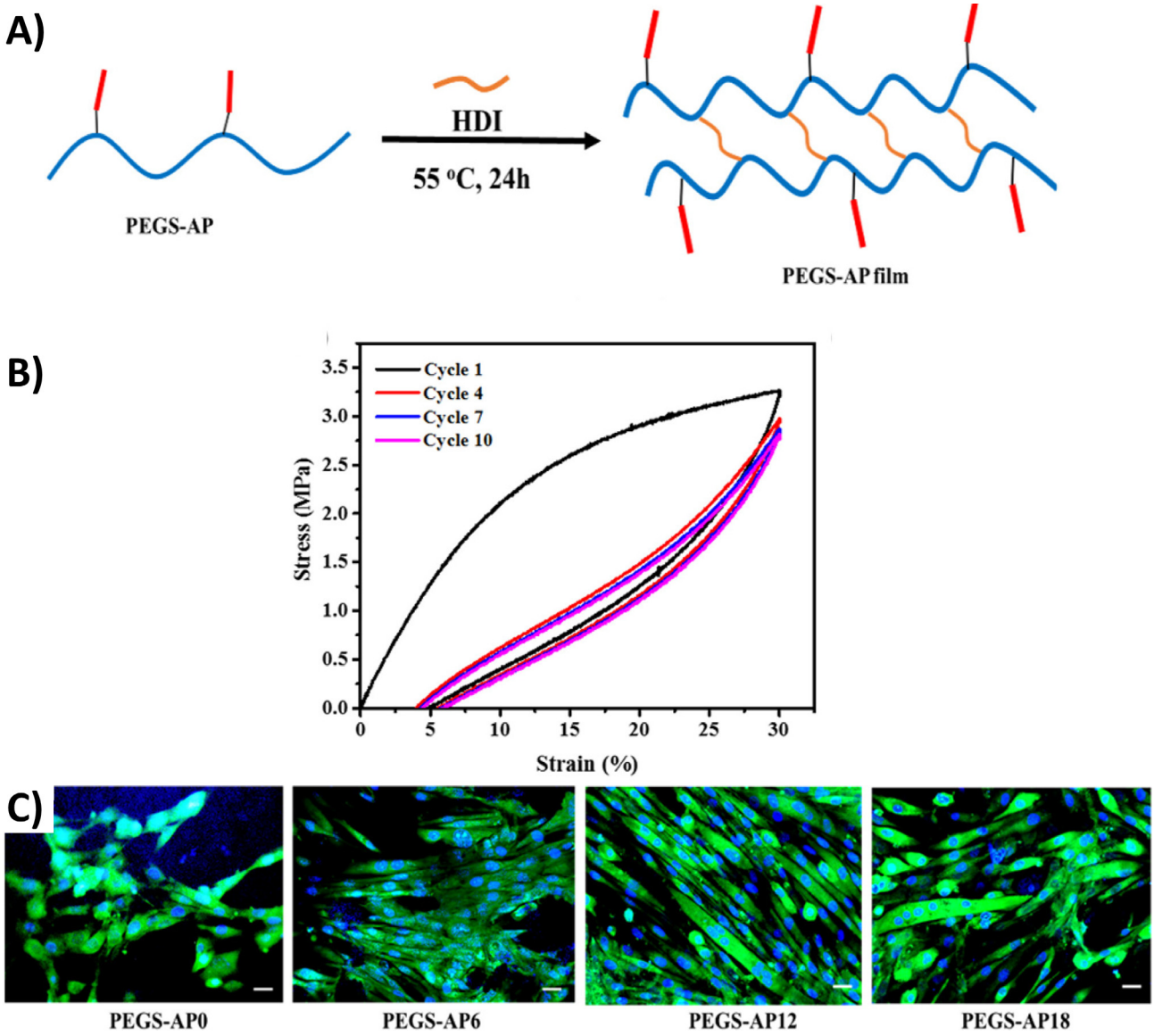

Fig. 7. A) Schematic representation of the PEGS-AP chemical structure. B) An example of cyclic tensile test results for a PEGS-AP film with 12 wt% AP. C) Influence of the AP weight percent on the differentiation of C2C12 cells. Reprinted from Dong *et. al.* [150] with permission from ACS publications, copyright 2017.

polydimethylsiloxane (PDMS) [152]. In this study, changing the ratio between PCL and PDMS resulted in changes in the shape behavior properties. *In vitro* studies with human fetal osteoblasts showed good proliferation of the cells and an increase in the expression of the ALP, a marker for osteogenic differentiation that indicates the beginning of bone matrix deposition [152]. A different type of shape memory scaffold was synthesized by copolymerizing PCL and poly(*iso*-butyl-morpholinedione) (PIBMD), a polydepsipeptide [153]. Incorporation of polydepsipeptides is thought to be advantageous for the degradation profile, whereas block copolymers with PCL show elastic behavior. Combining these two in a multiblock copolymer resulted in a shape memory material interesting for soft tissue implants.

4.2. Protein–protein hybrids

As mimicking the ECM in terms of both structure and function is a goal for tissue-engineered scaffolds, using natural ECM materials is a logical step. Electrospun cross-linked elastin and collagen scaffolds with different ratios were prepared [154]. By using collagen-to-elastin ratios of 1:1 and 9:1, it was shown that an increased ratio of elastin led to a reduction in both tensile strength and Young's modulus because the amine groups present were less and the crosslinking density was lower. *In vitro* cytocompatibility tests carried out with fibroblasts showed good proliferation of the cells on all scaffolds. It was also shown that myoblasts aligned and adhered to form myotubes in both 9:1 and 1:1 ratios of collagen to elastin scaffolds; however, on the 1:9 ratio of collagen to elastin scaffolds, the cells showed only round structures. Proliferation of the cells on the elastin-rich scaffolds was lower and thus limited the interactions between the cells, which is needed for differentiation. Cross-linked scaffolds of elastin and collagen were prepared for small-diameter blood vessel regeneration [155]. Introducing the crosslinks led to an increase in the stiffness of the scaffold compared to the non-cross-linked matrices, and *in vitro* cell studies on the cross-linked scaffolds showed expansion of smooth muscle cells during a 14-day culture period.

Precursors of native elastin and elastin derivatives have been used in combination with collagen for scaffold fabrication (Fig. 8A). Electrospun scaffolds of tropoelastin cross-linked with glutaraldehyde were analyzed by tensile testing in PBS at 37 °C (Fig. 8A) [156]. These tests showed that 50% or more collagen needed to be present compared to tropoelastin to provide the required mechanical properties. This is in line with the findings that small amounts of elastin can have a significant influence on the mechanical properties, as discussed in Section 2.3. For instance, the amount of elastin in the skin is approximately 2% of the tissue dry weight, but this amount has a significant impact on the elastic-

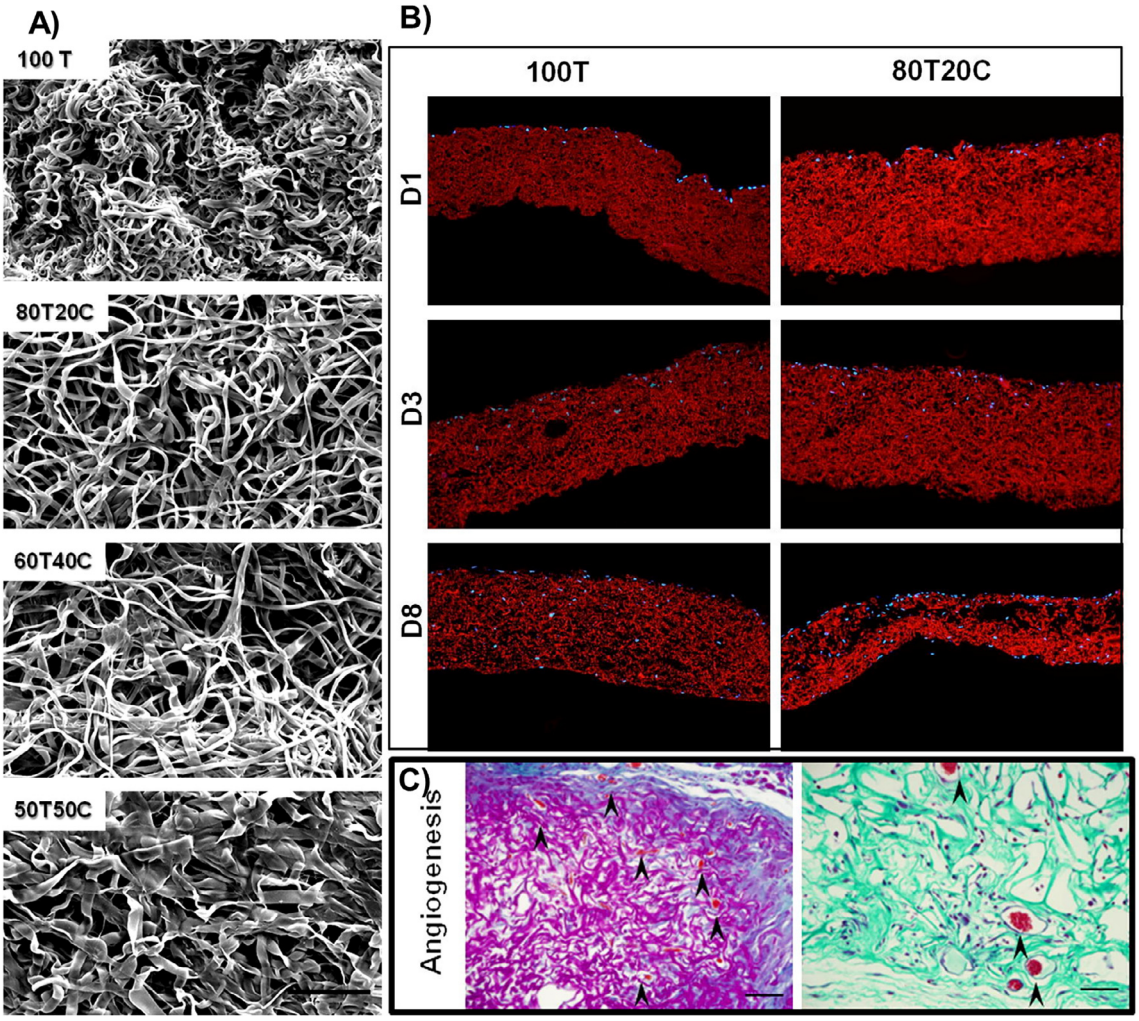

Fig. 8. A) Electrospun scaffolds with different ratios of tropoelastin/collagen. B) Fibroblast migration on two different scaffolds during *in vitro* studies for 8 days. C) Blood vessel formation after *in vivo* studies for 6 weeks for both the fabricated collagen-elastin scaffold (left) and the commercial Integra scaffold (right). Reprinted from Rnjak-Kovacina *et. al.* [156], with permission from Elsevier, copyright 2012.

ity of the tissue. It should be noted, however, that the structure of both collagen and elastin plays a crucial role with regard to this, meaning that only a small amount of elastin does not necessarily provide the proper elasticity that a tissue requires. Both *in vitro* and *in vivo* tests showed good mechanical integrity of the scaffold up to 6 weeks after subcutaneous implantation. In addition, fibroblast infiltration (Fig. 8B), deposition of new collagen matrix, and vascularization (Fig. 8C) within the newly formed tissue were observed [156]. In a different study, collagen was cross-linked using ELPs [157]. Although only a limited amount of data can be found on the mechanical properties of these scaffolds, it was indicated that the shear modulus increased relative to the concentration of the ELP, and *in vitro* tests showed reduced metabolic activity of fibroblasts compared to those cultured on pure collagen scaffolds. However, no difference in metabolic activity between endothelial cells and smooth muscle cells was found [157].

Elastin and elastin-like materials are often combined with silk fibroin or silk derivatives to form silk–elastin or silk–elastin-like polypeptides (SELPs). One example is the cross-linked silk fibroin–elastin scaffold [158], from which no mechanical characterization is available. However, the scaffolds showed high cell viability, and the presence of elastin increased the cell proliferation. Wound healing tests of the silk fibroin–elastin scaffold were carried out and compared with commercially available collagen dressings, and the results showed that scaffolds with a higher amount of elastin were able to induce keratinocyte and fibroblast migration [158]. Furthermore, the wounds were covered with a new layer of epithelium after 6 days of healing [158]. In another study, primary cortical neuron viability rates were used to study the feasibility of silk–tropoelastin scaffolds for neural tissue engineering [159]. Increasing the amount of tropoelastin improved the adhesion of the cells to the scaffold. However, using a scaffold with a high percentage of tropoelastin (50% or more) led to a high percentage of cell death, probably owing to the high positive net charge of the surface [159].

Moreover, silk derivatives were combined with the ELP using recombinant techniques to fabricate SELPs. These SELPs showed elasticity similar to that of the native elastin [160]. In addition, these SELPs were able to self-assemble into nanofibers [161,162]. Electrospun SELPs showed good mechanical properties, and *in vitro* cell viability and proliferation showed that SELPs could be a promising material for tissue engineering applications [163].

4.3. Synthetic polymer–protein scaffolds

As discussed in the previous sections, both synthetic and protein-based materials have their own advantages and disadvantages. To make use of all advantages, synthetic and protein-based materials can be combined into hybrid polymer–protein scaffolds. For example, to obtain an elastic scaffold, a block-*co*-polymer between PEG and a mimic of the hydrophilic-, alanine-, and lysine-rich parts of tropoelastin (AKELP) was made [164]. This PEG-AKELP showed compliant behavior until a strain of 10–15% under cyclic compression, after which stiffening occurred. The stress–strain curves overlapped by increasing the number of cycles and thus proved the elasticity of the scaffold. Cytotoxicity of PEG-AKELP was tested through indirect contact with porcine vocal cord fibroblasts, which showed no significant difference compared to the control. However, when direct cell studies were performed, good adhesion was not observed. In a later study, cell adhesion was improved by introducing an RGD motif onto the AKELP [165], which also influenced the mechanical properties.

PEG was introduced into an ELP scaffold to improve its transparency for 3D imaging [166]. However, it also influenced the functionalities of the scaffold. The presence of PEG increased the transition temperature of the LCST behavior but lowered the elastic modulus to 2.5 kPa compared to 5.6 kPa for a pure ELP hydrogel. Encapsulation studies of human fibroblasts into the ELP-PEG hydrogel showed 98% viability after both 4 and 7 days of culture [166]. To finely tune the mechanical properties of a complex water-soluble copolymer, containing poly(N-isopropylacrylamide) (PNIPAAm), polylactide-2-hydroxyethyl methacrylate (PLA-HEMA) and oligo (ethylene glycol) monomethyl (OEGMA), called PNPHO, was combined with elastin in different ratios [167]. Enhanced hydrophilicity by increasing the OEGMA ratio led to an increase in the gelling temperature, whereas an increased amount of the hydrophobic part (PLA-HEMA) led to a decrease in the gelling temperature. Finally, the gelling temperature could be tuned between 11 °C and 40 °C. The compression moduli of these hydrogels were between 40 and 150 kPa. Cell culture studies on the hydrogels showed cell viability of more than 80% immediately after cell encapsulation and showed good proliferation of cells after 5 days.

PLGA hybrids with elastin were also investigated for tissue engineering applications [168]. An increase in Young's modulus was found unexpectedly for the covalently linked PLGA-elastin. It was proven, however, that the change could be explained by the crosslinking of the PLGA fibers. The coupling reagents (1-ethyl-3-(3-dimethylaminopropyl, *N*-hydroxysuccinimide, and ethanesulfonic acid) used to covalently link PLGA to elastin are known to also crosslink PLGA. Thus, treating the PLGA with the same chemicals without the presence of elastin led to an increase in Young's modulus to 20.4 MPa, thus proving that the increase in Young's modulus is mainly due to the crosslinking of the PLGA. The differences in the 3D structure between the blended elastin-PLGA scaffold and the covalently linked PLGA-elastin are due to not only the covalent link between PLGA and elastin but also crosslinking; these materials were still compared in cell culture studies. Therefore, the influence of the covalent bond between elastin and PLGA and the influence of the crosslinking on the results of these cell studies remain unclear [168].

A hybrid material of thiol-functionalized hyaluronan and elastin prepared by using poly(ethylene glycol) diacrylate (PEGDA) as a crosslinker was assessed as a possible replacement for the nucleus pulposus of the intervertebral disc [169]. Although mechanical properties of these hydrogels were tunable, *in vivo* tests did not lead to a significant improvement in the patients [169]. As combining proteins and polymers through covalent bonds for tissue engineering has been recently started, many possibilities could still be investigated regarding the mechanical functionality and biological compatibility to obtain a complete picture of the potential of these materials for tissue engineering applications.

5. Discussion

The previous section provided an overview of different possibilities to introduce elasticity into tissue-engineered scaffolds with emphasis on the mechanical performance as well as the biological compatibility both *in vitro* and *in vivo*. All protein-based, synthetic, and hybrid materials exhibit interesting mechanical and biomedical functionalities, each with its own advantages and disadvantages (Table 7), thereby allowing for a fine-tuned solution for each application. The possibilities can be further extended by introducing biologically active components such as cell-penetrating motifs like RGD peptides [170–172]. Furthermore, different biological molecules could be combined with synthetic polymers such as a combination between submucosa and PU to obtain a scaffold for soft tissue engineering [173] or a combination between poly(isocyanopeptides) and DNA resulting in a hydrogel with properties tunable by external stimuli [174].

It is often difficult to compare the properties of different scaffolds. Mechanical analysis of the scaffolds is not always available,

Table 7
Advantages and disadvantages of different material categories for tissue engineering applications.

Material	Advantages	Disadvantages
Decellularized tissues	- Close mimic of the ECM structure of the native tissue [192]	- Limited applications owing to limits in the size and the shape [22] - Thorough purification is required, which needs optimization for each different tissue [193]
Purified insoluble elastin	- Biocompatible - Natural material [60]	- Purification often compromises functionality - Difficult to process [22]
Purified soluble elastin	- Biocompatible - Improved processability compared to insoluble elastin	- Large badge-to-badge variation
Tropoelastin	- Close mimic of elastin that can be obtained from nonanimal sources - Biocompatible	- Limited tunability
ELP	- Tunability of the construct - Biocompatible	- Short shelf-life - Thermal instability [194]
Synthetic elastomers	- Tunable mechanical properties - Size and shape can be varied.	- Lacking biological activity - Often, either good mechanical properties or preferable degradation
Polymer–polymer hybrids	- Combining the advantages of different synthetic polymers - Highly tunable	- Often lacking biological activity
Protein–protein hybrids	- Higher tunability of mechanical functionalities compared to single protein-based materials	- Thermal instability - Obtaining the components might be challenging
Polymer–protein hybrids	- Both biological and mechanical functionality present in the same material - Highly tunable mechanical functionality	- Synthesis might be challenging

and when available, experiments often have been carried out under different conditions. As explained in Section 2.2, elastin has a different mechanical behavior under wet conditions compared to dry conditions; the same would also probably apply to materials based on elastin. The Young's modulus of materials is not directly comparable because it is influenced by either the temperature, humidity, rate of the strain, relaxation time, or the type of the experiment. Furthermore, although Young's modulus gives an indication of elasticity, it is not sufficient to make conclusions for elasticity under noncyclic large strains. To prove this, cyclic stress–strain tests are of vital importance to provide a real indication of macroelastic behavior. However, some scaffolds with potential mechanical functionality for tissue engineering applications have yet to be evaluated using *in vitro* or *in vivo* studies to prove their biological compatibility for different targets.

Different measurement methods and different circumstances under which the measurements are carried out clearly lead to incomparability of the results. This becomes an issue when comparing different materials for a specific tissue engineering application. Therefore, it is crucial to set guidelines for each tissue engineering application with regard to the type of tests that need to be carried out. These tests should be performed under measurement circumstances that are comparable to the *in vivo* environment. The tests should cover both mechanical and biological evaluations, which will then lead to more cohesion and better comparability of the results.

In this review, introducing elastic components to the scaffolds is discussed. However, there are studies on how elastin production by cells and thus elasticity of the tissue-engineered constructs can be enhanced [11]. It has been shown that polyphenols increased the deposition of elastin by smooth muscle cells by enhancing the coacervation of tropoelastin; increasing lysyl oxidase synthesis, a crosslinking component; and inhibiting matrix metalloproteinase-2 activity that degrades elastin [175]. The addition of hyaluronan in combination with copper ions or transforming growth factor-β shows an increase in elastin production in adult rat smooth muscle cells [11,176]. In addition, heparin increased the elastin production in adult smooth muscle cells and fibroblasts as well as fetal cells [177].

Mechanical stimulation of tissue-engineered constructs also led to the increased elastin production [178–180]. However, these methods led to the presence of immature elastin, which does not result in the formation of an elastic matrix and is more prone to degradation by metalloproteinases and cathepsin S [181,182]. Moreover, the degradation products of immature elastin can cause calcification [183] and induce transformation of cell phenotypes, for example, from vascular smooth muscle cells to osteoblast-like cells [184]. It has been reported that fragments of elastin had an impact on inflammatory cells. For instance, elastin-derived peptides induced T-helper type 1 polarization of human blood lymphocytes [185]. Therefore, these shortcomings need to be considered when immature elastin is being introduced to the constructs *in vitro* or *in situ*.

It is important to note that for an implant to have long-term *in vivo* functionality, it should not only be mechanically and biologically functional upon implantation but also keep its function with time by maintaining a balance between the degradation rate of the scaffold and the formation of the neotissue. If the rate of the material degradation is significantly lower than the rate of the neotissue formation, it will result in calcification and fibrotic tissue formation at the implant site. However, if the material degradation is much faster than the neotissue formation, mechanical stability of the implant will be hampered [186]. Another important parameter to be addressed in the future studies is the spatial distribution of elastin. In many types of tissue, the amount and the structure of elastin differ spatially. This will lead to a tissue with heterogeneous mechanical properties, which is crucial for its proper *in vivo* functionality and thus has to be considered when designing the scaffolds.

Finally, smart materials are gaining interest for tissue engineering applications. For example, a wound dressing that could react to the environment by changing the permeability of the scaffold based on the moisture level of the wound was developed [187]. This self-changing ability could greatly increase the healing ability of the tissue. A shock-absorbent self-healing injectable scaffold was also synthesized to be used as an artificial nucleus pulposus of the intervertebral disc to improve the mechanical properties after implantation compared to nonhealing materials [188]. Combining these smart material functionalities with elastic materials could be the next step within the elastic tissue engineering field.

In conclusion, a combination of mechanical functionality, biological activity, and biocompatibility of the tissue-engineered

scaffold is of great importance for the translation of these methods into the clinic. Furthermore, these scaffolds should be able to maintain these mechanical and biological functions to provide long-term durability. To improve comparability of the different constructs, defining standard guidelines with regard to the measurement methods and conditions is necessary. Overall, the ability to introduce elasticity into the scaffolds increases the range of mechanical functionalities that can be fabricated and thus increases the potential applications for which the material can be used.

Acknowledgments

The authors acknowledge financial support from Aachen-Maastricht Institute for Biobased Materials (AMIBM), Maastricht University.

References

[1] Y. Ikada, Challenges in tissue engineering, J. R. Soc. Interface 3 (2006) 589–601.
[2] W.F. Daamen, J.H. Veerkamp, J.C. Van Hest, T.H. Van Kuppevelt, Elastin as a biomaterial for tissue engineering, Biomaterials 28 (2007) 4378–4398.
[3] R. Sodian, S.P. Hoerstrup, J.S. Sperling, S.H. Daebritz, D.P. Martin, F.J. Schoen, J. P. Vacanti, J.E.J. Mayer, Tissue engineering of heart valves: *in vitro* experiences, Ann. Thorac. Surg. 70 (2000) 140–144.
[4] B. Duan, L.A. Hockaday, K.H. Kang, J.T. Butcher, Aortic heart valves tissue regeneration, Tissue and Organ Regeneration (2014) 645–694.
[5] S. Ghazanfari, A. Khademhosseini, T.H. Smit, Mechanisms of lamellar collagen formation in connective tissues, Biomaterials 97 (2016) 74–84.
[6] S. Ghazanfari, A. Driessen-Mol, C.V.C. Bouten, F.P.T. Baaijens, Modulation of collagen fiber orientation by strain-controlled enzymatic degradation, Acta Biomater. 35 (2016) 118–126.
[7] S. Ghazanfari, A. Driessen-Mol, S.P. Hoerstrup, F.P.T. Baaijens, C.V.C. Bouten, Collagen matrix remodeling in stented pulmonary arteries after transapical heart valve replacement, Cells Tissues Organs 16 (2015) 159–169.
[8] K. Gulati, K.M. Poluri, Mechanistic and therapeutic overview of glycosaminoglycans: the unsung heroes of biomolecular signaling, Glycoconj. J. 33 (2016) 1–17.
[9] Y. Xue, V. Sant, J. Phillippi, S. Sant, Biodegradable and biomimetic elastomeric scaffolds for tissue-engineered heart valves, Acta Biomater. 48 (2017) 2–19.
[10] S. Ghazanfari, A. Driessen-Mol, B. Sanders, P.E. Dijkman, S.P. Hoerstrup, F.P.T. Baaijens, C.V.C. Bouten, *In vivo* collagen remodeling in the vascular wall of decellularized stented tissue-engineered heart valves, Tissue Eng. PT A 21 (2015) 2206–2215.
[11] C.B. Saitow, S.G. Wise, A.S. Weiss, J.J.J. Catellot, D.L. Kaplan, Elastin biology and tissue engineering with adult cells, Biomol Concepts 4 (2013) 173–185.
[12] A.M. Ruiz-Zapata, M.H. Kerkhof, S. Ghazanfari, B. Zandieh-Doulabi, R. Stoop, T. H. Smit, M.N. Helder, Vaginal fibroblastic cells from women with pelvic organ prolapse produce matrices with increased stiffness and collagen content, Sci. Rep. 6 (2016) 22971.
[13] S. Yi, F. Ding, L. Gong, X. Gu, Extracellular matrix scaffolds for tissue engineering and regenerative medicine, Curr. Stem Cell Res. Ther. 12 (2017) 233–246.
[14] D. Miranda-Nieves, E.L. Chaikof, Collagen and elastin biomaterials for the fabrication of engineered living tissues, ACS Biomater. Sci. Eng. 3 (2017) 694–711.
[15] L. Nivison-Smith, J. Rnjak, A.S. Weiss, Synthetic human elastin microfibers: stable cross-linked tropoelastin and cell interactive constructs for tissue engineering applications, Acta Biomater. 6 (2010) 354–359.
[16] K. Mendelson, F.J. Schoen, Heart valve tissue engineering: concepts, approaches, progress, and challenges, Ann. Biomed. Eng. 34 (2006) 1799–1819.
[17] S.G. Wise, A.S. Weiss, Tropoelastin, Int. J. Biochem. Cell Biol. 41 (2009) 494–497.
[18] P. Brown-Augsburger, C. Tisdale, T. Broekelmann, C. Sloan, R.P. Mecham, Identification of an elastin cross-linking domain that joins three peptide chains. Possible role in nucleated assembly, J. Biol. Chem. 270 (1995) 17778–17783.
[19] E.C. Davis, Stability of elastin in the developing mouse aorta: a quantitative radioautographic study, Histochemistry 100 (1993) 17–26.
[20] D.J. Johnson, P. Robson, Y. Hew, F.W. Keeley, Decreased elastin synthesis in normal development and in long-term aortic organ and cell cultures is related to rapid and selective destabilization of mRNA for elastin, Circ. Res. 77 (1995) 1107–1113.
[21] S.G. Wise, S.M. Mithieux, A.S. Weiss, Engineered tropoelastin and elastin-based biomaterials, Adv. Protein Chem. Struct. Biol. 78 (2009) 1–24.
[22] L. Nivison-Smith, A. Weiss, Elastin Based Constructs, Regenerative Medicine and Tissue engineering - Cells and Biomaterials (2011).
[23] L. Debelle, A.M. Tamburro, Elastin: molecular description and function, Int. J. Biochem. Cell Biol. 31 (1999) 261–272.
[24] R.S. Rapaka, K. Okamoto, D.W. Urry, Coacervation properties in sequential polypeptide models of elastin. Synthesis of H-(Ala-Pro-Gly-Gly)n-Val-OMe and H-(Ala-Pro-Gly-Val-Gly)n-Val-OMe, Int. J. Pept. Prot. Res. 12 (1978) 81–92.
[25] B. Vrhovski, A.S. Weiss, Biochemistry of tropoelastin, Eur. J. Biochem. 258 (1998) 1–18.
[26] P. Brown-Augsburger, T. Broekelmann, J. Rosenbloom, R.P. Mecham, Functional domains on elastin and microfibril-associated glycoprotein involved in elastic fibre assembly, Biochem. J. 318 (1996) 149–155.
[27] A.S. Narayanan, R.C. Page, F. Kuzan, C.G. Cooper, Elastin cross-linking *in vitro*. Studies on factors influencing the formation of desmosines by lysyl oxidase action on tropoelastin, Biochem. J. 173 (1978) 857–862.
[28] P.J. Baker, J.S. Haghpanah, J.K. Montclare, Elastin-based protein polymers, Polym. Biocatal. Biomater. II (2008) 37–51.
[29] M.B. van Eldijk, C.L. McGann, K.L. Kiick, J.C.M. van Hest, Elastomeric polypeptides, Top. Curr. Chem. 310 (2012) 71–116.
[30] L. Debelle, A.J.P. Alix, The structures of elastins and their function, Biochimie 81 (1999) 981–994.
[31] C.M. Bellingham, M.A. Lillie, J.M. Gosline, G.M. Wright, B.C. Starcher, A.J. Bailey, K.A. Woodhouse, F.W. Keeley, Recombinant human elastin polypeptides self-assemble into biomaterials with elastin-like properties, Biopolymers 70 (2003) 445–455.
[32] B.B. Aaron, J.M. Gosline, Elastin as a random-network elastomer: a mechanical and optical analysis of single elastin fibers, Biopolymers 20 (1981) 1247–1260.
[33] R.W. Carton, J. Dainauskas, J.W. Clark, Elastic properties of single elastic fibers, J. Appl. Physiol. 17 (1962) 547–551.
[34] J. Gosline, M. Lillie, E. Carrington, P. Guerette, C. Ortlepp, K. Savage, Elastic proteins: biological roles and mechanical properties, Phil. Trans. R. Soc. Lond. B 357 (2002) 121–132.
[35] S.M. Mithieux, A.S. Weiss, Elastin, Adv. Protein Chem. 70 (2005) 437–461.
[36] M.A. Gonzalez, J.R. Simon, A. Ghoorchian, Z. Scholl, S. Lin, M. Rubinstein, P. Marszalek, A. Chilkoti, G.P. López, X. Zhao, Strong, tough, strechable, and self-adhesive hydrogels from intrinsically unstructured proteins, Adv. Mater. 29 (2017) 1604743.
[37] E.M. Green, J.C. Mansfield, J.S. Bell, C.P. Winlove, The structure and micromechanics of elastic tissue, Interface Focus 4 (2014) 20130058.
[38] S. Fazaeli, S. Ghazanfari, V. Everts, T.H. Smit, J.H. Koolstra, The contribution of collagen fibers to the mechanical compressive properties of the temporomandibular joint disc, Osteoarthr. Cartil. 24 (2016) 1292–1301.
[39] R.I. Bashey, S. Torii, A. Angrist, Age-related collagen and elastin content of human heart valves, J. Gerontol. 22 (1967) 203–208.
[40] B.C. Starcher, Determination of the elastin content of tissues by measuring desmosine and isodesmosine, Anal. Biochem. 79 (1977) 11–15.
[41] I. Pasquali Ronchetti, M. Baccarani-Contri, Elastic fiber during development and aging, Microsc. Res. Tech. 38 (1997) 428–435.
[42] T.J. Peters, I.S. Smilie, Studies on chemical composition of meisci from the human knee-joint, Proc. R. Soc. Med. 64 (1971) 261–262.
[43] E.J. Bos, M. Pluemeekers, M. Helder, N. Kuzmin, K. Van Der Laan, M.L. Groot, G. Van Osch, P. Zuijlen, Structural and mechanical comparison of human ear, alar, and septal cartilage, Plast. Reconstr. Surg. 6 (2018) e1610.
[44] L. Nimeskern, L. Utomo, I. Lehtoviita, G. Fessel, J.G. Snedeker, G.J.V.M. Van Osch, R. Müller, K.S. Stok, Tissue composition regulates distinct viscoelastic responses in auricular and articular cartilage, J. Biomech. 49 (2016) 344–352.
[45] J. Liao, I. Vesely, Relationship between collagen fibrils, glycosaminoglycans, and stress relexation in mitral valve chordae tendineae, Ann. Biomed. Eng. 32 (2004) 977–983.
[46] J. Ritchie, J.N. Warnock, A.P. Yoganathan, Structural characterization of the chordae tendineae in native porcine mitral valves, Ann. Thorac. Surg. 80 (2005) 189–197.
[47] Y. Mikawa, H. Hamagami, J. Shikata, T. Yamamuro, elastin in the human intervertebral disk, Arch. Orthop. Trauma Surg. 105 (1985) 343–349.
[48] J.M. Cloyd, D.M. Elliott, Elastin content correlates with human disc degeneration in the anulus fibrosus and nucleus pulposus, Spine 32 (2007) 1826–1831.
[49] J. D'Armiento, Decreased elastin in vessel walls puts the pressure on, J. Clin. Invest. 112 (2003) 1308–1310.
[50] A.J.A. Leloup, C.E. Van Hove, A. Heykers, D.M. Schrijvers, G.R.Y. De Meyer, P. Fransen, Elastic and muscular arteries differ in structure, basal NO production and voltage-gated Ca2+-channels, Front. Physiol. (2015) 375.
[51] P.S. Clifford, S.R. Ella, A.J. Stupica, Z. Nourian, M. Li, L.A. Martinez-Lemus, K.A. Dora, Y. Yang, M.J. Davis, U. Pohl, G.A. Meininger, M.A. Hill, Spatial distribution and mechanical function of elastin in resistance arteries: a role in bearing longitudinal stress, Arterioscler. Thromb. Vasc. Biol. 31 (2011) 2889–2896.
[52] B. He, J.P. Wu, H.H. Chen, T.B. Kirk, J. Xu, Elastin fibers display a versatile microfibril network in articular cartilage depending on the mechanical environments, J. Orthop. Res. 31 (2013) 1345–1353.
[53] M. Scott, I. Vesely, Morphology of porcine aortic valve cusp elastin, J. Heart Valve Dis. 5 (1996) 464–471.
[54] I. Vesely, The role of elastin in aortic valve mechanics, J. Biomech. 31 (1998) 115–123.
[55] M. Scott, I. Vesely, Aortic valve cusp microstructure: the role of elastin, Ann. Thorac. Surg. 60 (1995) 391–394.
[56] I. Vesely, The role of elastin in aortic valve mechanics, J. Biomech. 31 (1997) 115–123.

[57] J. Melrose, S.M. Smith, R.C. Appleyard, C.B. Little, Aggrecan, versican and type VI collagen are components of annular translamellar crossbridges in the intervertebral disc, Eur. Spine J. 17 (2008) 314–324.
[58] H. Oxlund, J. Manschot, A. Viidik, The role of elastin in the mechanical properties of skin, J. Biomech. 32 (1988) 213–218.
[59] G.E. Amiel, M. Komura, O. Shapira, J.J. Yoo, S. Yazdani, J. Berry, S. Kaushal, J. Bischoff, A. Atala, S. Soker, Engineering of blood vessels from acellular collagen matrices coated with human endothelial cells, Tissue Eng. 12 (2006) 2355–2365.
[60] W.F. Daamen, T. Hafmans, J.H. Veerkamp, T.H. Van Kuppevelt, Isolation of intact elastin fibers devoid of microfibrils, Tissue Eng. 11 (2005) 1168–1176.
[61] S.M. Partridge, H.F. Davis, G.S. Adair, The chemistry of connective tissues. 2. Soluble proteins derived from partial hydrolysis of elastin, Biochem. J. 61 (1955) 11–21.
[62] R.B. Rucker, [36] Isolation of soluble elastin from copper-deficient chick aorta, Method Enzymol. 82 (1982) 650–657.
[63] N. Nakamura, T. Kimura, A. Kishida, Overview of the development, applications, and future perspectives of decellularized tissues and organs, ACS Biomater. Sci. Eng. 3 (2017) 1236–1244.
[64] C.E. Schmidt, J.M. Baier, Acellular vascular tissues: natural biomaterials for tissue repair and tissue engineering, Biomaterials 21 (2000) 2215–2231.
[65] A. Bader, G. Steinhoff, K. Strobl, T. Schilling, G. Brandes, H. Mertsching, D. Tsikas, J. Froelich, A. Haverich, Engineering of human vascular aortic tissue based on a xenogeneic starter matrix, Transplantation 70 (2000) 7–14.
[66] T.H. Petersen, E.A. Calle, L. Zhao, E.J. Lee, L. Gui, M.B. Raredon, K. Gavrilov, T. Yi, Z.W. Zhuang, C. Breuer, E. Herzog, L.E. Niklason, Tissue-engineered lungs for *in vivo* implantation, Science 329 (2010) 538–541.
[67] A.P. Price, K.A. England, A.M. Matson, B.R. Blazar, A. Panoskaltsis-Mortari, Development of a decellularized lung bioreactor system for bioengineering the lung: the matrix reloaded, Tissue Eng. Pt A 16 (2010) 2581–2591.
[68] A.L. Brown, W. Farhat, P.A. Merguerian, G.J. Wilson, A.E. Khoury, K.A. Woodhouse, 22 Week assessment of bladder acellular matrix as a bladder augmentation material in a porcine model, Biomaterials 23 (2002) 2179–2190.
[69] L. Du, X. Wu, Development and characterization of a full-thickness acellular porcine cornea matrix for tissue engineering, Artif. Organs 35 (2011) 691–705.
[70] T.H. Petersen, E.A. Calle, M.B. Colehour, L.E. Niklason, Matrix composition and mechanics of decellularized lung scaffolds, Cells Tissues Organs 195 (2012) 222–231.
[71] W. Gong, D. Lei, S. Li, P. Huang, Q. Qi, Y. Sun, Y. Zhang, Z. Wang, Z. You, X. Ye, Q. Zhao, Hybrid small-diameter vascular grafts: Anti-expansion effect of electrospun poly ε-caprolactone on heparin-coated decellularized matrices, Biomaterials 76 (2016) 359–370.
[72] T. Nguyen, C.A. Bashur, V. Kishore, Impact of elastin incorporation into electrochemically aligned collagen fibers on mechanical properties and smooth muscle cell phenotype, Biomed. Mater. 11 (2016) 025008.
[73] J. Rosenbloom, [9] Elastin: an overview, Method Enzymol. 144 (1987) 172–196.
[74] M. Li, M.J. Mondrinos, M.R. Gandhi, F.K. Ko, A.S. Weiss, P.I. Lelkes, Electrospun protein fibers as matrices for tissue engineering, Biomaterials 26 (2005) 5999–6008.
[75] H.A. Lucero, H.M. Kagan, Lysyl oxidase: an oxidative enzyme and effector of cell function, Cell. Mol. Life Sci. 63 (2006) 2304–2316.
[76] R.P. Mecham, Methods in elastic tissue biology: elastin isolation and purification, Methods 45 (2008) 32–41.
[77] L.B. Sandberg, T.B. Wolt, [37] Production and isolation of soluble elastin from copper-deficient swine, Method Enzymol. 82 (1982) 657–665.
[78] Z. Indik, W.R. Abrams, U.o. Kucich, C.W. Gibson, R.P. Mecham, J. Rosenbloom, Production of recombinant human tropoelastin: characterization and demonstration of immunologic and chemotactic activity, Arch. Biochem. Biophys. 280 (1990) 80–86.
[79] D. Bedell-Hogan, P. Trackman, W.R. Abrams, J. Rosenbloom, H.M. Kagan, Oxidation, cross-linking, and insolubilization of recombinant tropoelastin by purified lysyl oxidase, J. Biol. Chem. 268 (1993) 10345–10350.
[80] P.J. Stone, S.M. Morris, S. Griffin, S. Mithieux, A.S. Weiss, Building Elastin. Incorporation of recombinant human tropoelastin into extracellular matrices using nonelastogenic rat-1 fibroblasts as a source for lysyl oxidase, Am. J. Respir. Cell Mol. Biol. 24 (2001) 733–739.
[81] S.M. Mithieux, J.E.J. Rasko, A.S. Weiss, Synthetic elastin hydrogels derived from massive elastic assemblies of self-organized human protein monomers, Biomaterials 25 (2004) 4921–4927.
[82] J.D. White, S. Wang, A.S. Weiss, D.L. Kaplan, Silk-tropoelastin protein films for nerve guidance, Acta Biomater. 14 (2015) 1–10.
[83] D.W. Urry, M.M. Long, B.A. Cox, T. Ohnishi, L.W. Mitchell, M. Jacobs, The synthetic polypentapeptide of elastin coacervates and forms filamentous aggregates, Biochim. Biophys. Acta, Gen. Subj. 371 (1974) 597–602.
[84] A. Yeboah, R.I. Cohen, C. Rabolli, M.L. Yarmush, F. Berthiaume, Elastin-like polypeptides: a strategic fusion partner for biologics, Biotechnol. Bioeng. 113 (2016) 1617–1627.
[85] L.D. Muiznieks, S.E. Reichheld, E.E. Sitarz, M. Miao, F.W. Keeley, Proline-poor hydrophobic domains modulate the assembly and material properties of polymeric elastin, Biopolymers 103 (2015) 563–573.
[86] T. Tamura, T. Yamaoka, S. Kunugi, A. Panitch, D.A. Tirell, Effects of temperature and pressure on the aggregation properties of an engineered elastin model polypeptide in aqueous solution, Biomacromolecules 1 (2000) 552–555.
[87] D.M. Floss, K. Schallau, S. Rose-John, U. Conrad, J. Scheller, Elastin-like polypeptides revolutionize recombinant protein expression and their biomedical application, Trends Biotechnol. 28 (2010) 37–45.
[88] H. Betre, L.A. Setton, D.E. Meyer, A. Chilkoti, Characterization of a genetically engineered elastin-like polypeptide for cartilaginous tissue repair, Biomacromolecules 3 (2002) 910–916.
[89] D.L. Nettles, K. Kitaoka, N.A. Hanson, C.M. Flahiff, B.A. Mata, E.W. Hsu, A. Chilkoti, L.A. Setton, *In situ* crosslinking elastin-like polypeptide gels for application to articular cartilage repair in a goat osteochondral defect model, Tissue Eng. Pt A 14 (2008) 1133–1140.
[90] M.K. McHale, L.A. Setton, A. Chilkoti, Synthesis and *in vitro* evaluation of enzymatically cross-linked elastin-like polypeptide gels for cartilaginous tissue repair, Tissue Eng. 11 (2005) 1768–1779.
[91] Y.N. Zhang, R.K. Avery, Q. Vallmajo-Martin, A. Assmann, A. Vegh, A. Memic, B. D. Olsen, N. Annabi, A highly elastic and rapidly crosslinkable elastin-like polypeptide-based hydrogel for biomedical applications, Adv. Funct. Mater. 25 (2015) 4814–4826.
[92] E.R. Welsh, D.A. Tirrell, Engineering the extracellular matrix: a novel approach to polymeric biomaterials. I. Control of the physical properties of artificial protein matrices designed to support adhesion of vascular endothelial cells, Biomacromolecules 1 (2000) 23–30.
[93] D.L. Nettles, A. Chilkoti, L.A. Setton, Applications of elastin-like polypeptides in tissue engineering, Adv. Drug Deliver. Rev. 62 (2010) 1479–1485.
[94] J. Natarajan, Q. Dasgupta, S.N. Shetty, K. Sarkar, G. Madras, K. Chatterjee, Poly (ester amide)s from soybean oil for modulated release and bone regeneration, ACS Appl. Mater. Interfaces 8 (2016) 25170–25184.
[95] A. Leroy, A. Al Samad, X. Garric, S. Hunger, D. Noël, J. Coudane, B. Nottelet, Biodegradable networks for soft tissue engineering by thiol–yne photo cross-linking of multifunctional polyesters, RSC Adv. 4 (2014) 32017–32023.
[96] C.J. Bettinger, Biodegradable elastomers for tissue engineering and cell–biomaterial interactions, Macromol. Biosci. 11 (2011) 467–482.
[97] M.N. Abdallah, S. Abdollahi, M. Laurenti, D. Fang, S.D. Tran, M. Cerruti, F. Tamimi, Scaffolds for epithelial tissue engineering customized in elastomeric molds, J. Biomed. Mater. Res. B (2017).
[98] F.S. Mahdavi, A. Salehi, E. Seyedjafari, A. Mohammadi-Sangcheshmeh, A. Ardeshirylajimi, Bioactive glass ceramic nanoparticles-coated poly(l-lactic acid) scaffold improved osteogenic differentiation of adipose stem cells in equine, Tissue Cell 49 (2017) 565–572.
[99] L. Wang, Y. Wu, T. Hu, B. Guo, P.X. Ma, Electrospun conductive nanofibrous scaffolds for engineering cardiac tissue and 3D bioactuators, Acta Biomater. 59 (2017) 68–81.
[100] J.X. Chen, J. Yuan, Y.L. Wu, P. Wang, P. Zhao, G.Z. Lv, J.H. Chen, Fabrication of tough poly(ethylene glycol)/collagen double network hydrogels for tissue engineering, J. Biomed. Mat. Res. A 106A (2018) 192–200.
[101] J.J. Moon, M.S. Hahn, I. Kim, B.A. Nsiah, J.L. West, Micropatterning of poly (ethylene glycol) diacrylate hydrogels with biomolecules to regulate and guide endothelial morphogenesis, Tissue Eng. Pt A 15 (2009) 579–585.
[102] C.A. Sundback, J.Y. Shyu, Y. Wang, W.C. Faquin, R.S. Langer, J.P. Vacanti, T.A. Hadlock, Biocompatibility analysis of poly(glycerol sebacate) as a nerve guide material, Biomaterials 26 (2005) 5454–5464.
[103] I.S. Tobias, H. Lee, G.C.J. Engelmayr, D. Macaya, C.J. Bettinger, M.J. Cima, Zero-order controlled release of ciprofloxacin-HCl from a reservoir-based, bioresorbable and elastomeric device, J. Control. Release 146 (2010) 356–362.
[104] W.L. Neeley, S. Redenti, H. Klassen, S. Tao, T. Desai, M.J. Young, R. Langer, A microfabricated scaffold for retinal progenitor cell grafting, Biomaterials 29 (2008) 418–426.
[105] N. Masoumi, A. Jean, J.T. Zugates, K.L. Johnson, G.C.J. Engelmayr, Laser microfabricated poly(glycerol sebacate) scaffolds for heart valve tissue engineering, J. Biomed. Mater. Res. Part A 101A (2013) 104–114.
[106] P. Kerativitayanan, M. Tatullo, M. Khariton, P. Joshi, B. Perniconi, A.K. Gaharwar, Nanoengineered osteoinductive and elastomeric scaffolds for bone tissue engineering, ACS Biomater. Sci. Eng. 3 (2017) 590–600.
[107] X. Zhang, C. Jia, X. Qiao, T. Liu, K. Sun, Porous poly(glycerol sebacate) (PGS) elastomer scaffolds for skin tissue engineering, Polym. Test. 54 (2016) 118–125.
[108] B.G. Ilagan, B.G. Amsden, Surface modifications of photocrosslinked biodegradable elastomers and their influence on smooth muscle cell adhesion and proliferation, Acta Biomater. 5 (2009) 2429–2440.
[109] D. Motlagh, J. Allen, R. Hoshi, J. Yang, K. Lui, G. Ameer, Hemocompatibility evaluation of poly(diol citrate) *in vitro* for vascular tissue engineering, J. Biomed. Mater. Res. A 82A (2007) 907–916.
[110] A.R. Webb, V.A. Kumar, G.A. Ameer, Biodegradable poly(diol citrate) nanocomposite elastomers for soft tissue engineering, J. Mater. Chem. 17 (2007) 900–906.
[111] J.P. Santerre, K. Woodhouse, G. Laroche, R.S. Labow, Understanding the biodegradation of polyurethanes: from classical implants to tissue engineering materials, Biomaterials 26 (2005) 7457–7470.
[112] S.A. Guelcher, Biodegradable polyurethanes: synthesis and applications in regenerative medicine, Tissue Eng. Pt. B-Rev. 14 (2008) 3–17.
[113] Á.E. Mercado-Pagán, Y. Kang, D.F.E. Ker, S. Park, J. Yao, J. Bishop, Y. Yang, Synthesis and characterization of novel elastomeric poly(D, L-lactide urethane) maleate composites for bone tissue engineering, Eur. Polym. J. 49 (2013) 3337–3349.

[114] S. Grad, L. Kupcsik, K. Gorna, S. Gogolewski, M. Alini, The use of biodegradable polyurethane scaffolds for cartilage tissue engineering: potential and limitations, Biomaterials 24 (2003) 5163–5171.
[115] V. Chiono, P. Mozetic, M. Boffito, S. Sartori, E. Gioffredi, A. Silvestri, A. Rainer, S.M. Giannitelli, M. Trombetta, D. Nurzynska, F. Di Meglio, C. Castaldo, R. Miraglia, S. Montagnani, G. Ciardelli, Polyurethane-based scaffolds for myocardial tissue engineering, Interface Focus 4 (2014) 20130045.
[116] H.Y. Mi, X. Jing, M.R. Salick, L.S. Turng, X.F. Peng, Fabrication of thermoplastic polyurethane tissue engineering scaffold by combining microcellular injection molding and particle leaching, J. Mater. Res. 29 (2014) 911–922.
[117] H.Y. Mi, X. Jing, M.R. Salick, X.F. Peng, L.S. Turng, A novel thermoplastic polyurethane scaffold fabrication method based on injection foaming with water and supercritical carbon dioxide as coblowing agents, Polym. Eng. Sci. 54 (2014) 2947–2957.
[118] C. Xu, Y. Huang, J. Wu, L. Tang, Y. Hong, Triggerable degradation of polyurethanes for tissue engineering applications, ACS Appl. Mater. Interfaces 7 (2015) 20377–20388.
[119] P. Basnett, B. Lukasiewicz, E. Marcello, H.K. Gura, J.C. Knowles, I. Roy, Production of a novel medium chain length poly(3-hydroxyalkanoate) using unprocessed biodiesel waste and its evaluation as a tissue engineering scaffold, Microb. Biotechnol. 10 (2017) 1384–1399.
[120] S. Philip, T. Keshavarz, I. Roy, Polyhydroxyalkanoates: biodegradable polymers with a range of applications, J. Chem. Technol. Biot. 82 (2007) 233–247.
[121] D.B. Hazer, E. Kılıçay, B. Hazer, Poly(3-hydroxyalkanoate)s: Diversification and biomedical applications: a state of the art review, Mat. Sci. Eng. C 32 (2011) 637–647.
[122] S. Ghazanfari, A. Driessen-Mol, G.J. Strijkers, F.P.T. Baaijens, C.V.C. Bouten, The evolution of collagen fiber orientation in engineered cardiovascular tissues visualized by diffusion tensor imaging, PLoS ONE 10 (2015) e0127847.
[123] H. Kenar, G.T. Kose, M. Toner, D.L. Kaplan, V. Hasirci, A 3D aligned microfibrous myocardial tissue construct cultured under transient perfusion, Biomaterials 32 (2011) 5320–5329.
[124] N. Masoumi, D. Copper, P. Chen, A. Cubberley, K. Guo, R.Z. Lin, B. Ahmed, D. Martin, E. Aikawa, J. Melero-Martin, J. Mayer, Elastomeric fibrous hybrid scaffold supports *in vitro* and *in vivo* tissue formation, Adv. Funct. Mater. 27 (2017) 1606614.
[125] A. Mosahebi, P. Fuller, M. Wiberg, G. Terenghi, Effect of allogeneic schwann cell transplantation on peripheral nerve regeneration, Exp. Neurol. 173 (2001) 213–223.
[126] H.M. Chang, Z.H. Wang, H.N. Luo, M. Xu, X.Y. Ren, G.X. Zheng, B.J. Wu, X.H. Zhang, X.Y. Lu, F. Chen, X.H. Jing, L. Wang, Poly(3-hydroxybutyrate-co-3-hydroxyhexanoate)-based scaffolds for tissue engineering, Braz. J. Med. Biol. Res. 47 (2014) 533–539.
[127] L.R. Lizarraga-Valderrama, R. Nigmatullin, C. Taylor, J.W. Haycock, F. Claeyssens, J.C. Knowles, I. Roy, Nerve tissue engineering using blends of poly(3-hydroxyalkanoates) for peripheral nerve regeneration, Eng. Life Sci. 15 (2015) 612–621.
[128] S. Bhat, C. Chen, D.A. Day, Effects of a polycaprolactone (PCL) tissue scaffold in *rattus norvegicus* on blood flow, MRS Proceedings 1498 (2013) 27–31.
[129] S. Fleischer, R. Feiner, A. Shapira, J. Ji, X. Sui, H.D. Wagner, T. Dvir, Spring-like fibers for cardiac tissue engineering, Biomaterials 34 (2013) 8599–8606.
[130] P.J. Hanley, A.A. Young, I.J. LeGrice, S.G. Edgar, D.S. Loiselle, 3-Dimensional configuration of perimysial collagen fibres in rat cardiac muscle at resting and extended sarcomere lengths, J. Physiol. 517 (1999) 831–837.
[131] S. Arumuganathar, S.N. Jayasinghe, A versatile pressure assisted jet-fabrication by coating approach for forming biocompatible constructs for tissue engineering, Materials Lett. 62 (2008) 2574–2577.
[132] P. Sensharma, G. Madhumathi, R.D. Jayant, A.K. Jaiswal, Biomaterials and cells for neural tissue engineering: current choices, Mater. Sci. Eng. C Mater. Bio.l Appl. 77 (2017) 1302–1315.
[133] S.H. Lee, B.S. Kim, S.H. Kim, S.W. Choi, S.I. Jeong, I.K. Kwon, S.W. Kang, J. Nikolovski, D.J. Mooney, Y.K. Han, Y.H. Kim, Elastic biodegradable poly (glycolide-co-caprolactone) scaffold for tissue engineering, J. Biomed. Mat. Res. A 66A (2003) 29–37.
[134] A.P. Pêgo, A.A. Poot, D.W. Grijpma, J. Feijen, Copolymers of trimethylene carbonate and ε-caprolactone for porous nerve guides: synthesis and properties, J. Biomat. Sci-Polym. E 12 (2001) 35–53.
[135] A.P. Pêgo, C.L. Vleggeert-Lankamp, M. Deenen, E.A. Lakke, D.W. Grijpma, A.A. Poot, E. Marani, J. Feijen, Adhesion and growth of human Schwann cells on trimethylene carbonate (co)polymers, J. Biomed. Mater. Res. A 67A (2003) 876–885.
[136] S.K. Goswami, C.J. McAdam, L.R. Hanton, S.C. Moratti, Hyperelastic tough gels through macrocross-linking, Macromol. Rapid Commun. 38 (2017) 1700103.
[137] L. Navarro, N. Ceaglio, I. Rintoul, Structure and properties of biocompatible poly(glycerol adipate) elastomers modified with ethylene glycol, Polym. J. 49 (2017) 625–632.
[138] S. Ribeiro, P. Costa, C. Ribeiro, V. Sencadas, G. Botelho, S. Lanceros-Méndez, Electrospun styrene–butadiene–styrene elastomer copolymers for tissue engineering applications: effect of butadiene/styrene ratio, block structure, hydrogenation and carbon nanotube loading on physical properties and cytotoxicity, Compos. Part B-Eng 67 (2014) 30–38.
[139] S. Sant, D. Iyer, A.K. Gaharwar, A. Patel, A. Khademhosseini, Effect of biodegradation and *de novo* matrix synthesis on the mechanical properties of valvular interstitial cell-seeded polyglycerol sebacate-polycaprolactone scaffolds, Acta Biomater. 9 (2013) 5963–5973.
[140] S.H. Choi, T.G. Park, Synthesis and characterization of elastic PLGA/PCL/PLGA tri-block copolymers, J. Biomat. Sci-Polym. E 13 (2002) 1163–1173.
[141] A.P. Pêgo, A.A. Poot, D.W. Grijpma, J. Feijen, Physical properties of high molecular weight 1,3-trimethylene carbonate and D,L-lactide copolymers, J. Mater. Sci-Mater. M 14 (2003) 767–773.
[142] A.P. Pêgo, B. Siebum, M.J.A. Van Luyn, X.J. Gallego, Y. Van Seijen, A.A. Poot, D. W. Grijpma, J. Feijen, Preparation of degradable porous structures based on 1,3-trimethylene carbonate and D, L-lactide (co)polymers for heart tissue engineering, Tissue Eng. 9 (2003) 981–994.
[143] S.H. Kim, J.H. Kwon, M.S. Chung, E. Chung, Y. Jung, S.H. Kim, Y.H. Kim, Fabrication of a new tubular fibrous PLCL scaffold for vascular tissue engineering, J. Biomat. Sci-Polym. E 17 (2006) 1359–1374.
[144] S.I. Jeong, S.H. Kim, Y.H. Kim, Y. Jung, J.H. Kwon, B.S. Kim, Y.M. Lee, Manufacture of elastic biodegradable PLCL scaffolds for mechano-active vascular tissue engineering, J. Biomat. Sci-Polym. E 15 (2004) 645–660.
[145] S. Chung, N.P. Ingle, G.A. Montero, S.H. Kim, M.W. King, Bioresorbable elastomeric vascular tissue engineering scaffolds via melt spinning and electrospinning, Acta Biomater. 6 (2010) 1958–1967.
[146] S.H. Kim, E. Chung, S.H. Kim, Y. Jung, Y.H. Kim, S.H. Kim, A novel seamless elastic scaffold for vascular tissue engineering, J. Biomater. Sci-Polym. E 21 (2010) 289–302.
[147] K. Hassan, S.H. Kim, I. Park, S.H. Lee, S.H. Kim, Y. Jung, S.H. Kim, S.H. Kim, Small diameter double layer tubular scaffolds using highly elastic PLCL copolymer for vascular tissue engineering, Macromol. Res. 19 (2011) 122–129.
[148] Y. Jung, S.H. Kim, H.J. You, S.H. Kim, Y.H. Kim, B.G. Min, Application of an elastic biodegradable poly(L-lactide-co-ε-caprolactone) scaffold for cartilage tissue regeneration, J. Biomat. Sci-Polym. E 19 (2008) 1073–1085.
[149] Y. Jung, S.H. Lee, S.H. Kim, J.C. Lim, S.H. Kim, Synthesis and characterization of the biodegradable and elastic terpolymer poly(glycolide-co-L-lactide-co-ϵ-caprolactone) for mechano-active tissue engineering, J. Biomat. Sci-Polym. E 24 (2013) 386–397.
[150] R. Dong, X. Zhao, B. Guo, P.X. Ma, Biocompatible elastic conductive films significantly enhanced myogenic differentiation of myoblast for skeletal muscle regeneration, Biomacromolecules 18 (2017) 2808–2819.
[151] W. Sokolowski, A. Metcalfe, S. Hayashi, L. Yahia, J. Raymond, Medical applications of shape memory polymers, Biomed. Mater. 2 (2007) S23–27.
[152] D. Kai, M.P. Prabhakaran, B.Q.Y. Chan, S.S. Liow, S. Ramakrishna, F. Xu, X.J. Loh, Elastic poly(ε-caprolactone)-polydimethylsiloxane copolymer fibers with shape memory effect for bone tissue engineering, Biomed. Mater. 11 (2016) 015007.
[153] A. Battig, B. Hiebl, Y. Feng, A. Lendlein, M. Behl, Biological evaluation of degradable, stimuli-sensitive multiblock copolymers having polydepsipeptide- and poly(ε-caprolactone) segments in vitro, Clin. Hemorheol. Micro 48 (2011) 161–172.
[154] W.F. Daamen, H.T.B. Van Moerkerk, T. Hafmans, L. Buttafoco, A.A. Poot, J.H. Veerkamp, T.H. Van Kuppevelt, Preparation and evaluation of molecularly-defined collagen-elastin-glycosaminoglycan scaffolds for tissue engineering, Biomaterials 24 (2003) 4001–4009.
[155] L. Buttafoco, P. Engbers-Buijtenhuijs, A.A. Poot, P.J. Dijkstra, W.F. Daamen, T. H. Van Kuppevelt, I. Vermes, J. Feijen, First steps towards tissue engineering of small-diameter blood vessels: preparation of flat scaffolds of collagen and elastin by means of freeze drying, J. Biomed. Mat. Res. B 77B (2006) 357–368.
[156] J. Rnjak-Kovacina, S.G. Wise, Z. Li, P.K.M. Maitz, C.J. Young, Y. Wang, A.S. Weis, Electrospun synthetic human elastin:collagen composite scaffolds for dermal tissue engineering, Acta Biomater. 8 (2012) 3714–3722.
[157] Y. Garcia, N. Hemantkumar, R. Collighan, M. Griffin, J.C. Rodriguez-Cabello, A. Pandit, *In vitro* characterization of a collagen scaffold enzymatically cross-linked with a tailored elastin-like polymer, Tissue Eng. Part A 15 (2009) 887–899.
[158] A. Vasconcelos, A.C. Gomes, A. Cavaco-Paulo, Novel silk fibroin/elastin wound dressings, Acta Biomater. 8 (2012) 3049–3060.
[159] X. Hu, M.D. Tang-Schomer, W. Huang, X.X. Xia, A.S. Weiss, D.L. Kaplan, Charge-tunable autoclaved silk-tropoelastin protein alloys that control neuron cell responses, Adv. Funct. Mater. 23 (2013) 3875–3884.
[160] W. Teng, J. Cappello, X. Wu, Recombinant silk-elastinlike protein polymer displays elasticity comparable to elastin, Biomacromolecules 10 (2009) 3028–3036.
[161] S. Johnson, Y.K. Ko, N. Varongchayakul, S. Lee, J. Cappello, H. Ghandehari, S.B. Lee, S.D. Solares, J. Seog, Directed patterning of the self-assembled silk-elastin-like nanofibers using a nanomechanical stimulus, Chem. Commun. 48 (2012) 10654–10656.
[162] L. Zeng, L. Jiang, W. Teng, J. Cappello, Y. Zohar, X. Wu, Engineering aqueous fiber assembly into silk-elastin-like protein polymers, Macromol. Rapid Commun. 35 (2014) 1273–1279.
[163] R. Machado, A. Da Costa, V. Sencadas, C. Garcia-Arévalo, C.M. Costa, J. Padrão, A. Gomes, S. Lanceros-Méndez, J.C. Rodríguez-Cabello, M. Casal, Electrospun silk-elastin-like fibre mats for tissue engineering applications, Biomed. Materials 8 (2013) 065009.
[164] S.E. Grieshaber, A.J.E. Farran, S. Lin-Gibson, K.L. Kiick, X. Jia, Synthesis and characterization of elastin–mimetic hybrid polymers with multiblock, alternating molecular architecture and elastomeric properties, Macromolecules 42 (7) (2009) 2532–2541.
[165] S.E. Grieshaber, A.J.E. Farran, S. Bai, K.L. Kiick, X. Jia, Tuning the properties of elastin mimetic hybrid copolymers via a modular polymerization method, Biomacromolecules 13 (2012) 1774–1786.

[166] H. Wang, L. Cai, A. Paul, A. Enejder, S.C. Heilshorn, Hybrid elastin-like polypeptide-polyethylene glycol (ELP-PEG) hydrogels with improved transparency and independent control of matrix mechanics and cell ligand density, Biomacromolecules 15 (2014) 3421–3428.
[167] A. Fathi, S.M. Mithieux, H. Wei, W. Chrzanowski, P. Valtchev, A.S. Weiss, F. Dehghani, Elastin based cell-laden injectable hydrogels with tunable gelation, mechanical and biodegradation properties, Biomaterials 35 (2014) 5425–5435.
[168] Z.I. Foraida, T. Kamaldinov, D.A. Nelson, M. Larsen, J. Castracane, Elastin-PLGA hybrid electrospun nanofiber scaffolds for salivary epithelial cell self-organization and polarization, Acta Biomater. 62 (2017) 116–127.
[169] I.L. Moss, L. Gordon, K.A. Woodhouse, C.M. Whyne, A.J.M. Yee, A novel thiol-modified hyaluronan and elastin-like polypetide composite material for tissue engineering of the nucleus pulposus of the intervertebral disc, Spine 36 (2011) 1022–1029.
[170] G.R. Alas, R. Agarwal, D.M. Collard, A.J. García, Peptide-functionalized poly [oligo(ethylene glycol) methacrylate] brushes on dopamine-coated stainless steel for controlled cell adhesion, Acta Biomater. 59 (2017) 108–116.
[171] J. Usprech, D.A. Romero, C.H. Amon, C.A. Simmons, Combinatorial screening of 3D biomaterial properties that promote myofibrogenesis for mesenchymal stromal cell-based heart valve tissue engineering, Acta Biomater. 58 (2017) 34–43.
[172] S. Ravi, J.M. Caves, A.W. Martinez, C.A. Haller, E.L. Chaikof, Incorporation of fibronectin to enhance cytocompatibility in multilayer elastin-like protein scaffolds for tissue engineering, J. Biomed. Mater. Res. A 101A (2013) 1915–1925.
[173] L. Da, M. Gong, A. Chen, Y. Zhang, Y. Huang, Z. Guo, S. Li, J. Li-Ling, L. Zhang, H. Xie, Composite elastomeric polyurethane scaffolds incorporating small intestinal submucosa for soft tissue engineering, Acta Biomater. 59 (2017) 45–57.
[174] S.R. Deshpande, R. Hammink, F.H.T. Nelissen, A.E. Rowan, H.A. Heus, Biomimetic stress sensitive hydrogel controlled by DNA nanoswitches, Biomacromolecules 18 (2017) 3310–3317.
[175] A. Sinha, N. Nosoudi, N. Vyavahare, Elasto-regenerative properties of polyphenols, Biochem. Biophys. Res. Commun. 444 (2014) 205–211.
[176] T.C. Rothuizen, R. Kemp, J.M.G.J. Duijs, H.C. De Boer, R. Bijkerk, E.P. Van Der Veer, L. Moroni, A.J. Zonneveld, A.S. Weiss, T.J. Rabelink, J.I. Rotmans, Promoting tropoelastin expression in arterial and venous vascular smooth muscle cells and fibroblasts for vascular tissue engineering, Tissue Eng. PT C 22 (2016) 923–931.
[177] C. Baughman, D.L. Kaplan, J.J. Castellot Jr., Heparin stimulates elastogenesis: application to silk-based vascular grafts, Matrix Biol. 30 (2011) 346–355.
[178] M.C. Sutcliffe, J.M. Davidson, Effect of static stretching on elastin production by porcine aortic smooth muscle cells, Matrix 10 (1990) 148–153.
[179] M. Wanjare, N. Agarwal, S. Gerecht, Biomechanical strain induces elastin collagen production in human pluripotent stem cell-derived vascular smooth muscle cells, Am. J. Physiol. Cell Physiol. 15 (2015) 271–281.
[180] J.H. Eoh, N. Shen, J.A. Burke, S. Hinderer, Z. Xia, K. Shenke-Layland, S. Gerecht, Enhanced elastin synthesis and maturation in human vascular smooth muscle tissue derived from induced-pluripotent stem cells, Acta Biomater. 52 (2017) 49–59.
[181] C. Ntayi, A.L. Labrousse, R. Debret, P. Birembaut, G. Bellon, F. Antonicelli, W. Hornebeck, P. Bernard, Elastin-derived peptides upregulate matrix metalloproteinase-2-mediated melanoma cell invasion through elastin-binding protein, J. Invest. Dermatol. 122 (2004) 256–265.
[182] E.R. Smith, L.A. Tomlinson, M.L. Ford, L.P. McMahon, C. Rajkumar, S.G. Holt, Elastin degradation is associated with progressive aortic stiffening and all-cause mortality in predialysis chronic kidney disease, Hypertension 59 (2012) 973–978.
[183] A. Pai, E.M. Leaf, M. El-Abbadi, C.M. Giachelli, Elastin degradation and vascular smooth muscle cell phenotype change precede cell loss and arterial medial calcification in a uremic mouse model of chronic kidney diseas, Am. J. Pathol. 178 (2011) 764–773.
[184] N. Hosaka, M. Mizobuchi, H. Ogata, C. Kumata, F. Kondo, F. Koiwa, E. Kinugasa, T. Akizawa, Elastin degradation accelerates phosphate-induced mineralization of vascular smooth muscle cells, Calcif. Tissue Int. 85 (2009) 523–529.
[185] T.L. Adair-Kirk, R.M. Senior, Fragments of extracellular matrix as mediators of inflammation, Int. J. Biochem. Cell Biol. 40 (2008) 1101–1110.
[186] T. Sugiura, S. Tara, H. Nakayama, T. Yi, Y.U. Lee, T. Shoji, C.K. Breuer, T. Shinoka, Fast-degrading bioresorbable arterial vascular graft with high cellular infiltration inhibits calcification of the graft, J. Vasc. Surg. 66 (2017) 243–250.
[187] R. Gharibi, H. Yeganeh, H. Gholami, Z.M. Hassan, Aniline tetramer embedded polyurethane/siloxane membranes and their corresponding nanosilver composites as intelligent wound dressing materials, RSC Adv. 4 (2014) 62046–62060.
[188] A. Pérez-San Vincente, M. Peroglio, M. Ernst, P. Casuso, I. Loinaz, H.J. Grande, M. Alini, D. Eglin, D. Dupin, Self-healing dynamic hydrogel as injectable shock-absorbing artificial nucleus pulposus, Biomacromolecules 18 (2017) 2360–2370.
[189] A.P. Bonartsev, G.A. Bonartseva, K.V. Shaitan, M.P. Kirpichnikov, Poly(3-hydroxybutyrate) and poly(3-hydroxybutyrate)-based biopolymer systems, Biochem. (Moscow) Suppl. Ser. B Biomed. Chem. 5 (2011) 10–21.
[190] A.P. Pêgo, A.A. Poot, D.W. Grijpma, J. Feijen, Biodegradable elastomeric scaffolds for soft tissue engineering, J. Control. Release 87 (2003) 69–79.
[191] S.I. Jeong, B.S. Kim, Y.M. Lee, K.J. Ihn, H.S. Kim, Y.H. Kim, Morphology of elastic poly(l-lactide-*co*-ε-caprolactone) copolymers and in vitro and in vivo degradation behavior of their scaffolds, Biomacromolecules 5 (2004) 1303–1309.
[192] K.P. Robb, A. Shridhar, L. Flynn, Decellularized matrices as cell-instructive scaffolds to guide tissue-specific regeneration, ACS Biomater. Sci. Eng. (2017).
[193] S. Hinderer, S.L. Layland, K. Schenke-Layland, ECM and ECM-like materials—Biomaterials for applications in regenerative medicine and cancer therapy, Adv. Drug Deliver. Rev. 97 (2016) 260–269.
[194] D. Chow, M.L. Nunalee, D.W. Lim, A.J. Simnick, A. Chilkoti, Peptide-based biopolymers in biomedicine and biotechnology, Mater. Sci. Eng. R Rep. 62 (2008) 125–155.